HELSINKI UNIVERSITY OF TECHNOLOGY
Faculty of Electronics, Communications and Automation
Department of Communications and Networking

UPLINK POWER CONTROL IN RELAY ENHANCED LTE ADVANCED NETWORKS

AYDIN KARAER

Thesis submitted in partial fulfillment of the requirements for the Degree of Master of Science in Radio Communications

Espoo, March 2009

Supervisor: Professor Jyri Hämäläinen

Instructor: Doc. Simone Redana

ABSTRACT

Author:	Aydin Karaer
Name of Thesis:	UPLINK POWER CONTROL IN RELAY ENHANCED LTE ADVANCED NETWORKS
Date:	March 5, 2009 **Number of Pages:** 83
Faculty:	Faculty of Electronics, Communication and Automation
Department:	Department of Communications and Networking
Supervisor:	Prof. Jyri Hämäläinen
Instructor:	Doc. Simone Redana

In April 2008, the 3rd Generation Partnership Project (3GPP) agreed on its candidate technology named as LTE Advanced (LTE-A) to fulfill the requirements of IMT Advanced which was recently defined by ITU. According to the requirements, LTE-A is expected to provide high data rates while maintaining coverage proportional to LTE Release 8.

In this thesis, a novel way of implementing the relaying concept is proposed to satisfy the tough demands of LTE-A as relays improve cell edge capacity, lower OPEX, reduce backhaul costs and enhance network topology. This thesis discusses the positive and negative aspects of deployment of relays within the LTE framework and evaluates the performance of relay enhanced cells (REC). Moreover, the new cell edges introduced by relay nodes (RN) will lead to severe intra-cell and inter-cell interference, in particular, when a high number of RNs are deployed in the cell with reuse one.

Power control (PC) becomes an important method for mitigating this interference as well as increasing the cell edge and system capacity in the uplink (UL). Hence, the standardized 3GPP LTE UL PC scheme should be investigated in relay based deployment. This thesis mainly examines the UL in RECs within the LTE framework in terms of LTE UL PC scheme that considers a fractional PC in which performance enhancement is aimed for the cell center users by inducing an acceptable level of inter-cell interference.

Furthermore, the thesis includes an investigation of parameter configuration and performance evaluation of the LTE UL PC in Macro cell scenarios. Subsequently, the 3GPP's approved UL PC scheme for LTE is applied both at eNBs and RNs in relay based deployment and performance evaluation is given. Parameter optimization and transmit power setup are examined to achieve optimal performance in REC scenarios.

Keywords: 3GPP, LTE, LTE Advanced, Relay, Uplink, Power Control

PREFACE

This Master's Thesis presents the work that was carried out under the supervision of Prof. Jyri Hämäläinen from Helsinki University of Technology (HUT) and under the instruction of Doc. Simone Redana from Nokia Siemens Networks (NSN). The thesis work was performed at NSN premises in Munich / Germany from June 2008 to January 2009.

ACKNOWLEDGMENTS

I would like to thank my supervisor Jyri Hämäläinen for his guidance and encouragement throughout the course of this thesis. I believe that without his understanding and cooperation this work would not have been so successful. I also would like to thank my instructor Simone Redana for his effort and patience on me from the first day till the end. I think that we managed to work well as a team. Special thanks also go to Bernhard Raaf, Michel Juergen and Ingo Viering for their constructive feedback and support.

Furthermore, I also send my special thanks to all my former Nokia Siemens Networks colleagues sitting in the same room with me, who shared the lunch breaks and also dinners at different restaurants.

I would like to thank Anzil Abdul Rasheed for his support at work and friendship during my stay in Germany. Tommaso Beniero and Abdallah Bou Saleh also deserve my gratitude for their cooperation and friendship. William Martin has a right to have my gratitude as well for his valuable support in the language of the thesis.

Finally, a loving thank you to my parents for their invaluable help during my different moods, making me feel more responsible and giving me focus in my life.

March, 2009

Espoo, Finland

Aydin Karaer

TABLE OF CONTENTS

LIST OF ACRONYMS and NOTATIONS

ACRONYMS

1G	1^{st} Generation
2G	2^{nd} Generation
3G	3^{rd} Generation
3GPP	3rd Generation Partnership Project
4G	4^{th} Generation
AF	Amplify-and-Forward
AMC	Adaptive Modulation and Coding
BER	Bit Error Rate
BS	Base Station
BSC	Base Station Controller
CAPEX	Capital Expenditure
CDF	Cumulative Distribution Function
CDMA	Code Division Multiple Access
CLPC	Closed Loop Power Control
CP	Cyclic Prefix
D-AMPS	Digital Advanced Mobile Phone System
DF	Decode-and-Forward
DVB	Digital Video Broadcasting
DwPTS	Downlink Pilot Time Slot
EDGE	Enhanced Date Rates for GSM Evolution
eNodeB	Base Transceiver Station in LTE
EPC	Evolved Packet Core
E-UTRAN	Evolved UMTS Terrestrial Radio Access Network
FCPC	Full Compensation Power Control
FDD	Frequency Division Duplex
FFT/IFFT	Fast Fourier Transform / Inverse Fast Fourier Transform
FPC	Fractional Power Control
GGSN	Gateway GPRS Support Node
GI	Guard Interval
GP	Guard Period
GPRS	General Packet Radio Service
GSM	Global System for Mobile Communications
HARQ	Hybrid Automatic Repeat Request
HII	High Interference Indication
HLR	Home Location Register

HSDPA	High-Speed Downlink Packet Access
HSPA	High-Speed Packet Access
HSPA+	Evolved HSPA
HSS	Home Subscriber Server
HSUPA	High-Speed Uplink Packet Access
ICI	Inter-carrier Interference
IDFT/DFT	Inverse Discrete Fourier Transform / Discrete Fourier Transform
IMS	IP Multimedia Subsystem
IMT	International Mobile Telecommunications
ISD	Inter Site Distance
ISI	Inter-symbol Interference
ITU	International Telecommunication Union
LTE	Long Term Evolution
LTE-A	LTE Advanced
MBMS	Multimedia Broadcast/Multicast Service
MCS	Modulation and Coding Scheme
MIMO	Multiple Input Multiple Output
MME	Mobility Management Entity
MMS	Multimedia Message Service
MS	Mobile Station
NodeB	Base Transceiver Station in UMTS
OFDM	Orthogonal Frequency Division Multiplexing
OFDMA	Orthogonal Frequency Division Multiple Access
OI	Overload Indication
OLPC	Open Loop Power Control
OPEX	Operational Expenditure
PAPR	Peak to average Power Ratio
PC	Power Control
PCRF	Policy and Charging Rules Function
PDCCH	Physical Downlink Control Channel
PDCP	Packet Data Converge Protocol
PDN	Public Data Network
PRB	Physical Resource Block
PSD	Power Spectral Density
PRACH	Packet Random Access Channel
PUCCH	Physical Uplink Control Channel
PUSCH	Physical Uplink Shared Channel
QAM	Quadrature Amplitude Modulation

QoS	Quality of Service
QPSK	Quadrature Phase Shift Keying
REC	Relay Enhanced Cell
RLC	Radio Link Control
RN	Relay Node
RNC	Radio Network Controller
RR	Round Robin
RRC	Radio Resource Control
RRM	Radio Resource Management
SAE	System Architecture Evaluation
SC-FDMA	Single Carrier Frequency Division Multiple Access
SGI	Signaling Gateway Interface
SGSN	Serving GPRS Support Node
S-GW	Serving Gateway
SINR	Signal to Interference + Noise Ratio
SMS	Short Message Service
TDD	Time Division Duplex
TTI	Transmission Time Interval
UE	User Equipment
UMTS	Universal Mobile Telecommunication Services
UpPTS	Uplink Pilot Time Slot
VoIP	Voice over Internet Protocol
WCDMA	Wideband Code Division Multiple Access
WIMAX	Worldwide Interoperability for Microwave Access
WINNER	Wireless World Initiative New Radio
WLAN	Wireless Local Area Network

NOTATIONS

$\boldsymbol{\alpha}$	Cell specific pathloss compensation factor
$\boldsymbol{IoT}$	Interference over thermal noise
$\boldsymbol{L}$	Downlink pathloss estimated at UE
$\boldsymbol{M}$	Number of allocated PRBs to a UE
$\boldsymbol{N}$	Thermal noise
$\boldsymbol{P}$	UE transmit power
$\boldsymbol{P}_0$	Power contained in one PRB (defines SINR target)
$\boldsymbol{P}_{\mathbf{max}}$	Maximum allowed UE transmit power

LIST OF FIGURES

LIST OF TABLES

1 INTRODUCTION

The foundation of wireless communication was initiated by transmission of three-dot Morse code over a distance of three kilometers by Guglielmo Marconi in 1895. Tremendous development has taken place in wireless communication systems from that time right up to the present day. The concept of cellular mobile communication was introduced through first generation analog networks that were deployed in the early 1980s. Second generation (2G) technologies Global Mobile System (GSM) in Europe and Digital Advanced Mobile Phone System (D-AMPS) in the US were taken into use from 1991 onwards. These second generation systems improved greatly on their predecessors in terms of digital encryption, higher capacity, and digital data services such as Short Message Service (SMS) and better Quality of Service (QoS).

Later, the GSM system was improved by General Packet Radio Service (GPRS) supporting up to 114 Kbits/s and Enhanced Data Rates for GSM Evolution (EDGE) supporting up to 384 Kbits/s by means of packet switching and higher order modulation schemes. Due to the introduction of Universal Mobile Telecommunication Services (UMTS) third generation (3G) networks, data rates up to 2 Mbits/s and user services such as Multimedia Message Service (MMS), Internet browsing and file transferring were supported. Wideband Code Division Multiple Access (WCDMA) and its evolution High-Speed Downlink Packet Access (HSDPA) makes 14.4 Mbits/s data rates possible in downlink transmission, while High-Speed Uplink Packet Access (HSUPA) makes 5.76 Mbits/s date rates possible in uplink transmission.

Currently, 3G UMTS networks are mostly being upgraded to High Speed Packet Access (HSPA) which refers to the two existing standards, HSDPA and HSUPA. Further enhancements are being introduced through HSPA+ which was initially described in 3rd Generation Partnership Project’s (3GPP) Release 7 in 2007 supporting an all-IP architecture and data rates up to 42 Mbit/s in the downlink and 22 Mbit/s in the uplink by means of Multiple Input Multiple Output (MIMO) technologies and higher order modulation. In HSPA it is already possible to browse the Internet, watch videos and listen to music by using 3G phones.

In parallel with HSPA evolution, the 3GPP has started a project named 3G Long Term Evolution (LTE) to improve the present standards to be able to cope with future requirements. The initial requirements of the LTE were set in Release 7 where target peak data rates of 100 Mbits/s in downlink and 50 Mbits/s in uplink were introduced. The requirements for LTE also aim for average user throughput which is 3-4 times higher than what HSDPA offers in the downlink and 2-3 times higher than what HSUPA offers in the uplink. The LTE is also expected to meet the demand for better coverage, improved spectrum efficiency and reduced delays. To achieve these targets, different air interface techniques were proposed and examined.

As a consequence, Orthogonal Frequency Division Multiple Access (OFDMA) was adopted to the LTE downlink and Single Carrier Frequency Division Multiple Access (SC-FDMA) to the LTE uplink. These access methods were selected due to, for example, high immunity to inter-symbol interference, good bandwidth scalability and superior spectral efficiency. Furthermore, the standardization of LTE in 3GPP has reached a mature level and the latest set of 3GPP standards with Release 8 are expected to be ready during 2009. These standards will collect the completion of 3GPP Release 7 HSPA+ features, voice over HSPA, Common IP Multimedia Subsystem (IMS) and LTE standards. The 3G LTE networks are anticipated to be deployed from 2010 onwards as a natural evolution of GSM and UMTS networks [14].

However, the 3G LTE does not meet the requirements of International Mobile Telecommunication (IMT) Advanced that were recently defined by International Telecommunication Union (ITU). Therefore in April 2008, 3GPP agreed on its candidate technology named as *LTE Advanced* (LTE-A) to fulfill the requirements of IMT Advanced. The first set of requirements on LTE-A were described with a technical report [15] in June 2008. Due to backward compatibility, LTE-A should be considered not as a revolution but more as an evolution to LTE. It is comparable to LTE with improved features to enhance the system, deployment and cost related requirements. The LTE-A also promises to support peak data rates of 1 Gbits/s in downlink and 500 Mbits/s in uplink transmission, bandwidth scalability up to 100 MHz, and to improve user and control plane latencies, VoIP capacity and performance at the cell edge.

The standardization process of LTE-A has already started and the first standard is expected to be ready in 3GPPs' Release 10. Deployment of LTE-A networks is anticipated to happen approximately sometime between 2012 and 2015 as an upgrade to LTE. The proposal phase is ongoing for LTE-A to meet the defined target requirements. Initial proposals have been submitted and currently many working groups are contributing to the progress.

1.1 Problem statement

In particular, future wireless communication systems are operating above the 2 GHz carrier frequency which results in a heavy pathloss in radio transmission. According to the requirements, LTE-A is expected to provide high data rates while maintaining coverage proportional to LTE Release 8 without an unrealistic increase in transmission powers. However, aggressive propagation conditions restrict the radio coverage especially in urban areas. An increase in transmit power would be a solution to this problem with the cost of higher interference in the network and shorter battery lifetime in terminals. Another solution would be to deploy more base stations which in turn would lead to higher deployment and maintenance costs since the number of subscribers may not grow proportionally. In any case, these solutions cannot provide better performance for the cell edge users.

In order to satisfy high throughput and coverage requirements, *relay nodes* (RN) provide an attractive solution for LTE-A. *Relaying* concept can efficiently improve cell edge capacity, lower OPEX expenses, reduce backhaul costs and enhance network topology which are all the demands of LTE-A. One purpose of this thesis is to discuss the possible positive and negative aspects of this implementation of relaying concept in LTE framework and carry out a performance evaluation for a *Relay Enhanced Cell (REC)*. It is noted that heterogeneous cell deployment with low power relay nodes requires detailed dimensioning and planning. New cell edges introduced by RNs will lead to severe intra-cell and inter-cell interference in particular when a high number of relay nodes is deployed in the cell with reuse one.

Power control (PC) becomes an important means in the uplink transmission to mitigate the interference and increase the cell edge and system capacity. Therefore, the original LTE power control scheme should be re-investigated in relay based deployment to achieve an optimal performance. The main purpose of this thesis is to investigate the uplink power control in REC within the LTE framework. The 3GPP's approved uplink power control scheme for LTE is applied in relay based deployment and its performance evolution is given. Further performance enhancement is achieved with parameter tuning and feasible transmit power configurations.

1.2 Research approach and assessment methodology

1.2.1 Research approach

This thesis work aims to investigate the performance of the REC and to find an optimal solution for power control in the REC. The following steps will be taken to achieve the goal:

- Literature study of LTE uplink transmission scheme based on SC-FDMA
- Theoretical study of relaying concept from related works
- Creation of system level simulator for LTE uplink transmission investigations in REC
- Definition of power control parameter configurations in Macro cell scenarios
- Power control optimization and system performance evaluation in REC

1.2.2 Assessment methodology

Performance evaluation of different scenarios and different optimized configurations are performed based on some Key Performance Indicators (KPI) that will be given as:

- *User Throughput*: is the experienced throughput per user in the uplink transmission
- *X % ile User Throughput*: is the throughput at the X % ile point of the Cumulative Distribution Function (CDF) of the user throughput. It is used to show the coverage performance
- *Cell capacity*: is the total throughput of users per transmission time interval in the uplink
- *Average IoT*: is the total received interference power divided by the thermal noise. It is used to describe the Interference
- *SINR per PRB*: is the experienced Signal to Noise + Interference Ratio (SINR) at each Physical Resource Block (PRB) of uplink resource grid

- *UE Tx Power*: is the transmit power of a user

A simplified static simulation approach is followed to obtain and assess the KPIs by the system level snap-shot simulator.

1.3 Main limits in the scope of the thesis

Some limitations on the scope of the thesis are discussed here:

- Only uplink transmission is considered.
- This thesis investigates Frequency Division Duplex (FDD) only and assumes an ideal relay link. A complete REC scenario is also carried out using combined FDD-TDD mode and performance evaluation is given in Appendix F.
- Advanced antenna techniques that are used in 3GPP LTE such as Multiple Input Multiple Output (MIMO) are not considered. However, the system level simulator takes into account the multiple antennas at access points as defined in [18] and the corresponding transmitter and receiver diversity gains.
- Only open loop power control (OLPC) is applied. Thus, open loop parameters that are specified in the 3GPP LTE uplink power control formula are considered and closed loop corrections are omitted.
- Parameters and assumptions are adopted from the latest text proposal for the LTE Advanced evaluation methodology [18].

1.4 Thesis outline

Chapter 2 contains a literature review which describes 3GPP LTE features by focusing on LTE requirements and used transmission schemes. The uplink transmission methodology is reviewed in detail.

In Chapter 3 the targets of LTE-A are given and one of the proposed catalysts of LTE-A, an implementation of relaying concept, is covered with its positive and negative aspects. Heterogeneous cell deployment is described.

The rationale behind power control as well as power control schemes for different technologies such as GSM, WCDMA and HSPA are discussed in Chapter 4. Additionally, the simulator description is given, the LTE uplink fractional power control is examined extensively and its performance evaluation is shown.

The performance analysis of REC is included in Chapter 5, where power control is studied in the REC scenario. Parameter optimization and maximum allowed transmit power settings are introduced to obtain optimal performance and the results achieved are discussed.

In Chapter 6, the work is briefly summarized and conclusions are drawn. This chapter closes with recommendations for further study to continue building upon the achievements of this present Master’s thesis.

2 INTRODUCTION TO LTE

This chapter introduces 3GPP's *Long Term Evolution* work which is expected to ensure a competitive edge over other radio technologies. The LTE is the latest standard of the 3GPP mobile network technologies which include GSM, GPRS, WCDMA and HSPA. It started during the early GSM times with Release 98, which was continued with Release 99 that specified the first Universal Mobile Telecommunication Services (UMTS), 3G networks with a CDMA air interface. It was then followed by the all-IP core network enhancement of WCDMA in Release 4 (Release 2000) which was the standardization phase of 3GPP up to the year 2001.

Presently, the UMTS networks are mostly being upgraded to HSPA which was firstly introduced in 3GPP's Release 5 as HSDPA in 2002, subsequently as HSUPA in Release 6 in 2004 in order to obtain an increased data rate and capacity. The evolution is ongoing with HSPA+, which was initially described in Release 7 in 2007, and accompanied by LTE Release 8 expected in 2009.

The LTE radio access, called Evolved UMTS Terrestrial Radio Access Network (E-UTRAN), is supposed to enhance the user throughputs and system capacity, reduce user plane latency as well as introducing improved user satisfaction with full mobility. End-to-end Quality of Service (QoS) targets will be maintained with entirely IP-based traffic support, and also Voice over IP (VoIP) will be integrated with other multimedia services. This chapter includes a discussion on LTE design targets and requirements. An overview of LTE radio access, network architecture and LTE transmission schemes is also presented.

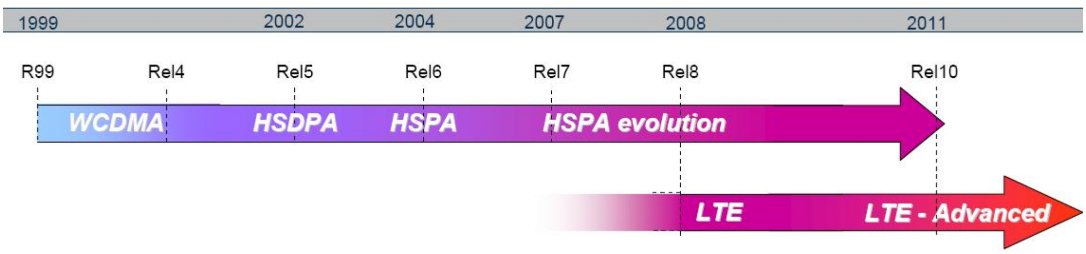

Figure 2-1 LTE evolution

2.1 LTE design targets and requirements

The first step of the LTE requirements and targets were set and documented by 3GPP already in 3GPP TR 25.913 [1] Release 7. Targets and requirements for LTE are listed and briefly explained here.

2.1.1 Capabilities

Peak data rate

A peak data rate of 100 Mbps in the downlink and 50 Mbps in the uplink within a 20 MHz spectrum is targeted.

Duplexing scheme

As a duplexing scheme, LTE supports both FDD and TDD operation. It is clear that peak data rate requirements cannot be satisfied with TDD due to the lack of simultaneous transmission for downlink and uplink. This, however, can be obtained with a FDD scheme.

Latency

Latency requirements are different for user plane and control plane. A user plane latency of 5 ms in one-way is necessary. Control plane latencies are measured according to two different transitions. The control plane latency of 50 ms of transition time from a dormant state to an active state is needed. The dormant state is a state where the terminal is unknown to the network and no radio resources are assigned. The control plane latency of 100 ms of transition time from a camped state to an active state is required. The camped state is a state where the terminal is known to the network and the network is aware of which cell the terminal is in but no radio resources have yet been assigned.

2.1.2 System performance

In general, the performance requirements of LTE are expressed comparative to the baseline system using Release 6 HSPA.

Throughput

As an objective in the downlink LTE, a 3-4 times higher average throughput than Release 6 HSDPA and a 2-3 times higher throughput than Release 6 HSDPA at the cell edge (5 % ile user throughput) are targeted. In addition, for the uplink LTE, a 2-3 times higher average throughput than Release 6 Enhanced Uplink and a 2-3 times higher average throughput than Release 6 Enhanced Uplink at the cell edge (5 % ile user throughput) are aimed.

Spectrum efficiency

In the downlink, a 3-4 times higher spectral efficiency than Release 6 HSDPA and in the uplink a 2-3 times higher spectral efficiency than Release 6 Enhanced Uplink are among the targets.

Mobility

Optimal performance is targeted for the terminal speeds between 0-15km/h. High performance is maintained from 15km/h up to 120km/h. Connection should be kept up to 350km/h and even up to 500km/h depending on the frequency band.

Coverage

Cell ranges up to 5 km should meet the performance targets (throughput, spectral efficiency and mobility) mentioned above. Cell ranges up to 30 km should meet the performance targets mentioned above with minor degradations in throughput and spectrum efficiency. There are no mandatory specifications for cell ranges up to 100 km.

2.1.3 Deployment Aspects

Scenarios

Deployment scenario requirements for LTE should meet both a stand alone system and an interworking system which works together with WCDMA/HSPA and/or GSM.

Spectrum flexibility

1.25 MHz, 1.6 MHz, 2.5 MHz, 5 MHz, 10 MHz, 15 MHz and 20 MHz spectrum allocations should be supported for both TDD mode and FDD mode.

Complexity and cost

The new deployment should be able to use the existing infrastructure such as base station locations and be compatible with the earlier defined releases. Complexity and power consumption of UEs should be minimized. Therefore, Operational Expenditure (OPEX) and Capital Expenditure (CAPEX) should be kept as small as possible.

A whole packet switched architecture

Development of a fully packet based architecture is also one of the requirements in LTE. One trend in future will be that circuit switched calls will not exist and voice calls will be based on VoIP.

2.2 LTE radio access and network architecture

2.2.1 Radio access

The LTE downlink and uplink transmission schemes are defined as OFDMA and SC-FDMA respectively by 3GPP. Reasons that make the OFDMA the preferred solution for the LTE radio access will be listed in the sections below.

Bandwidth flexibility and simple receiver design

The LTE has a target for high bit rates using large bandwidth, up to 20 MHz, whereas the UMTS spectrum allocation in WCDMA/HSPA only stands 5 MHz bandwidth usage with an optimum performance when equalizers are used at the receivers. Even with the system bandwidth increases in LTE, the OFDMA overcomes the multipath components by means of maintained signal orthogonality whereas CDMA suffers from multipath components. It results in a more complex receiver design to solve the components for CDMA. Consequently, bandwidth flexibility in OFDMA is much higher compared to CDMA and it permits a simpler receiver design.

Flat architecture

During the architecture development in HSPA, more intelligence was added to the system. UMTS was already defined as a hierarchical architecture in which the radio functionalities were located at the Radio Network Controller (RNC). In the flat architecture of LTE, however, all radio related functions that are needed for fast packet scheduling are located in the base station. Thus, a fast frequency domain scheduling which results in up to 50% capacity improvement can be applied in an OFDMA scheme but not in CDMA, where the interference is spread over the whole bandwidth.

Benefits of SC-FDMA

In OFDMA, the Peak-to-Average Power Ratio (PAPR) of the transmitted signal requires a good linearity in the transmitter power amplifier. However, linear amplifiers have low efficiency and thus, in the uplink where mobile terminals aim to minimize their power consumption, OFDMA is not the optimum solution. Instead, SC-FDMA which allows a better usage of power amplifiers is chosen for the uplink transmission in LTE.

Simplified multi-antenna usage

The targeted high bit rates in LTE can be achieved by using large bandwidth and multiple antennas. In LTE, MIMO antenna technologies can be implemented in a simpler way than in CDMA based systems.

2.2.2 Network architecture

The overall network architecture of LTE can be found in [4]. An illustration of the overall network structure is given in Figure 2-2.

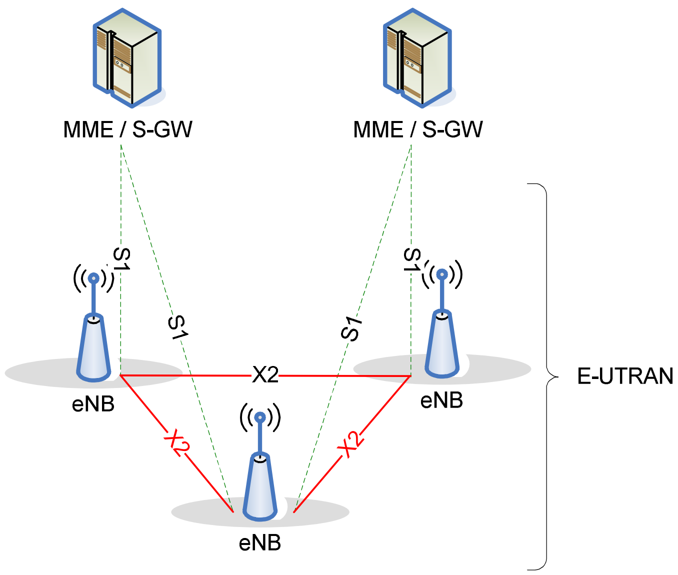

Figure 2-2 Overall LTE network architecture

The E-UTRAN consists of base stations that are called as e-NodeBs (eNB). These eNBs provide E-UTRA user plane (contains PDCP, RLC, MAC and PHY) and control plane (contains RRC) protocol terminations towards UEs. The eNBs are interconnected with each other via an X2 interface and the eNBs are also connected via an S1 interface to the Evolved Packet Core (EPC), more specifically to the Mobility Management Entity (MME) and to the Serving Gateway (S-GW). The S1 interface supports multiple relations between MMEs / S-GWs and eNBs.

In LTE, radio functionalities are moved to base stations. New functionalities such as Radio Resource Control (RRC), Radio Link Control (RLC) and the Packet Data Convergence Protocol (PDCP) are introduced additional to HSPA.

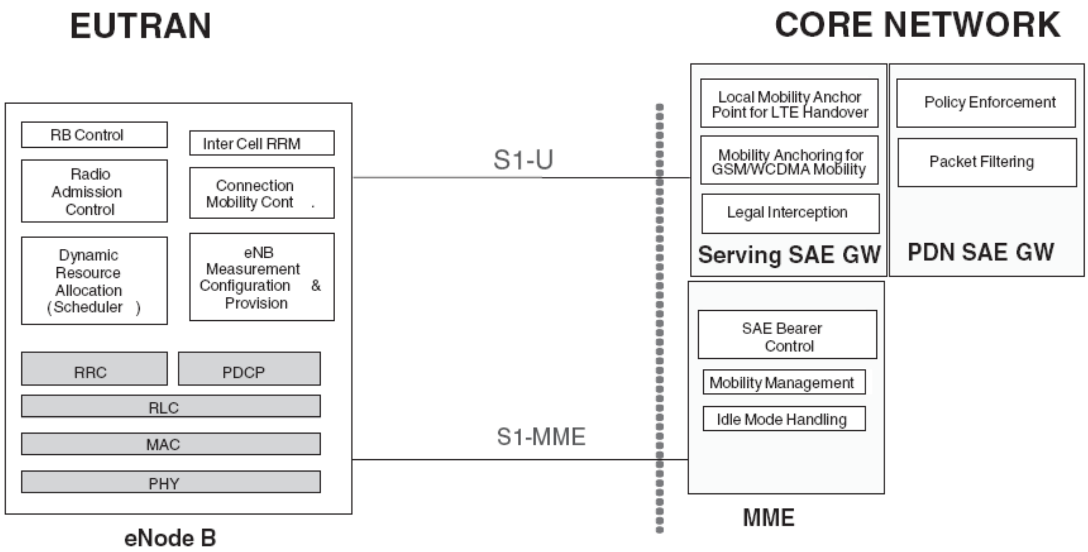

Figure 2-3 Functional structure of radio access and core network in LTE [2]

While Release 6 includes four network elements in the user and the control plane such as base station, RNC, SGSN (Serving GPRS Support Node) and GGSN (Gateway GPRS Support Node), the Release 8 LTE aims to have only two network elements such as the base station in the radio network and the Access Gateway (a-GW) in the core network. New radio access does not support soft handover in the system which greatly simplifies the implementation. This approach has been also used in HSDPA and was inherited by LTE.

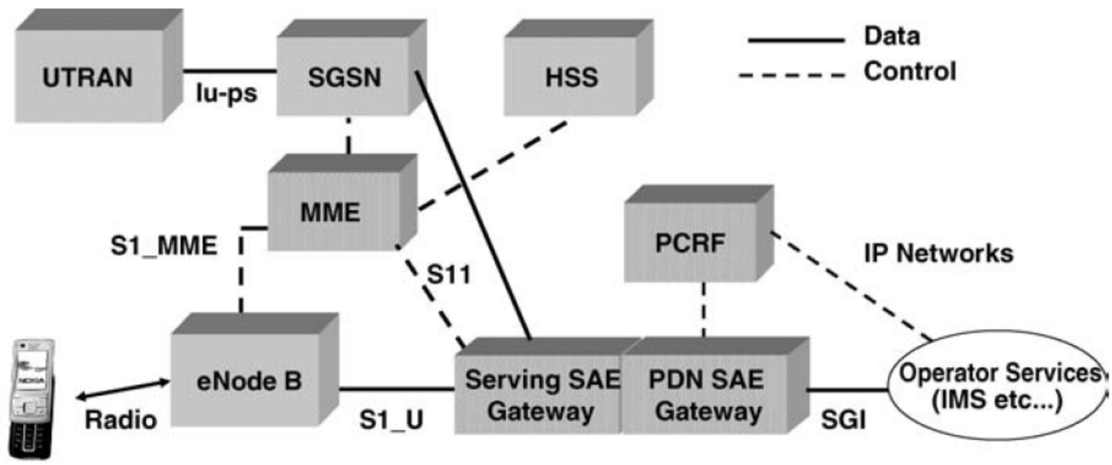

Figure 2-4 LTE / System architecture evolution (SAE) [2]

More detailed 3GPP core network system architecture is given in Figure 2-4. The E-UTRAN eNodeB functionalities and important functionalities of core network entities are listed briefly as follows:

The functions of the *eNodeB* are Radio Resource Management, IP header compression and encryption of user data streams, routing of user plane data towards the serving gateway, scheduling and transmission of paging messages as well as measurement and measurement reporting configuration for mobility and scheduling.

The *Serving SAE Gateway* (S-GW) and the *Public Data Network* (PDN) *SAE Gateway* (P-GW) are responsible for the mobility management inside the LTE network as well as between the other 3GPP radio technologies such as GSM and UMTS. The responsibility of the S-GW is to report the Local Mobility Anchor point for inter-eNB handover and to manage the inter-3GPP mobility, packet routing and forwarding. The functions of the P-GW include per-user based packet filtering, UE IP address allocation and uplink and downlink service level charging, gating and rate enforcement.

The *Mobility Management Entity* (MME) manages the control place signaling for idle state mobility handling and mobility management. Security control and SAE Bearer control are also performed by MME. Finally, the MME and SAE/PDN gateways are connected via the S11 interface.

The *Home Subscriber Server* (HSS) replaces the old Home Location Register (HLR) and covers its functionalities such as providing a database of user specific information on service priorities and data rates.

The *Policy and Charging Rules Function* (PCRF) is responsible for the charging policy and QoS policies.

2.3 LTE transmission schemes

As already mentioned, the downlink transmission scheme for E-UTRAN LTE is defined as OFDMA, whereas the uplink transmission scheme is based on SC-FDMA. In this section, the basics of OFDM, OFDMA and SC-FDMA are described. The uplink transmission scheme is explained extensively due to the fact that the focus of this current research lies there.

2.3.1 OFDM, OFDMA and SC-FCDMA

Orthogonal Frequency Division Multiplexing (OFDM) is the chosen radio technology to meet the requirements of 3GPP LTE as it has been used for WLAN, WIMAX and broadcast technologies like DVB. The OFDM has aroused the interest recently due to its capabilities of allowing high data rate transmission in multipath channels that occur in frequency selective fading environments. It introduces the usage of smaller frequency bands that are assigned to subcarriers and transmitting with lower rates instead of transmitting over the whole frequency band. Furthermore, OFDM uses the orthogonal subcarrier overlapping to exploit the used bandwidth as efficiently as possible.

Different subcarriers maintain the orthogonality between each other because at the same sampling instant of a single subcarrier, the other subcarriers have a zero value.

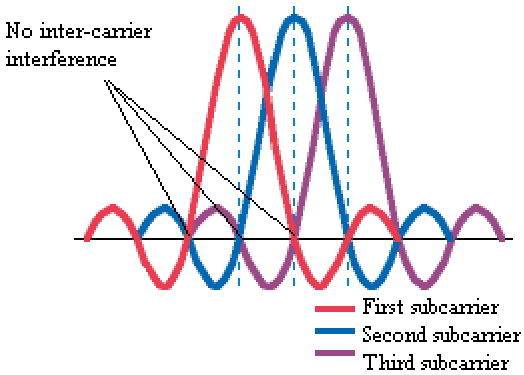

Figure 2-5 OFDM subcarrier spectrum

This kind of subcarrier spacing eliminates the inter-carrier interference (ICI) without considering the multipath transmission. On the other hand, multipath channel environment with different fading characteristics alters the orthogonality of the subcarriers of the OFDM symbol.

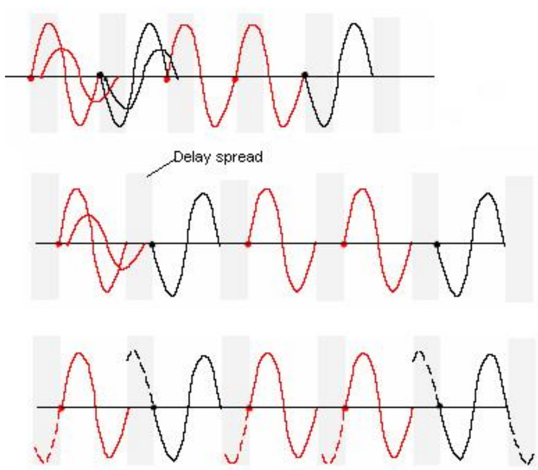

Figure 2-6 Cyclic prefix addition illustration [5]

The same multipath phenomena also gives rise to the delay spread in the transmission and consequently delayed versions of the signals lead to an inter-symbol interference (ISI). This can be compensated for by moving the symbols further from the region of delay spread as can be seen in Figure 2-6; however from the hardware point of view, this is not applicable. We can, therefore, extend the symbol period by adding the copy of the last samples of the symbol to the beginning part of the symbol. This part is called the Cyclic Prefix (CP) and the delay spread region is known as the Guard Interval (GI). It should be noted that the CP addition comes at the cost of additional power and increased bandwidth requirements.

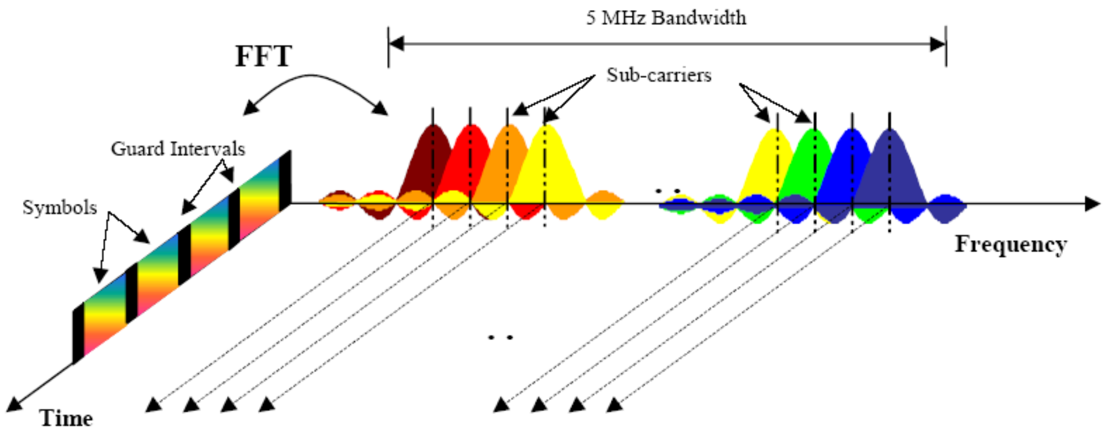

Figure 2-7 Frequency-time representation of an OFDM signal

Figure 2-7 adopted from [6] illustrates the OFDM Signal. It shows a signal with 5 MHz bandwidth. However, the principle for other E-UTRA bandwidths is the same. Data symbols are independently modulated and transmitted over a high number of closely spaced orthogonal subcarriers.

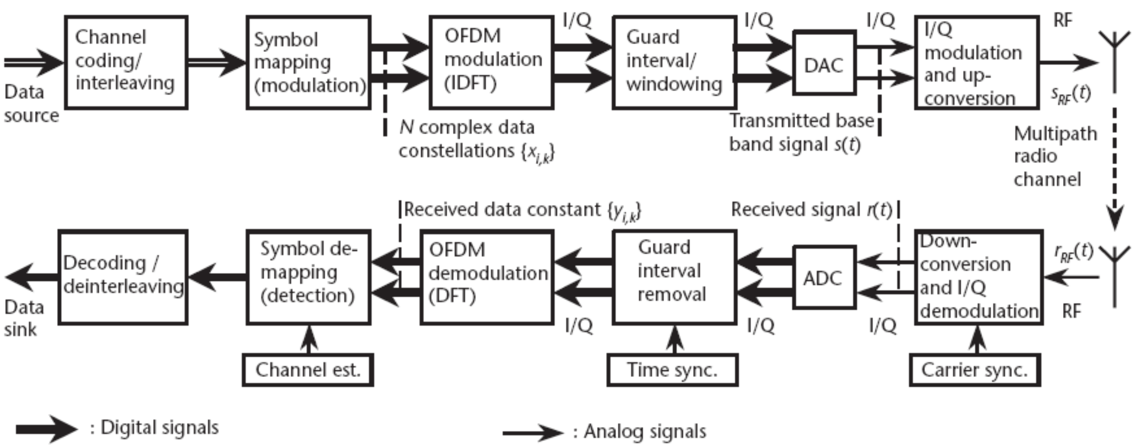

Figure 2-8 OFDM transmitter and receiver [7]

In practice, the OFDM signals can be generated using Inverse Fast Fourier Transform (IFFT) and demodulated using Fast Fourier Transform (FFT) digital signal processing techniques. Firstly, the OFDM subcarriers are assigned to some data symbols to transmit, and, the amplitude and phase of the subcarriers are determined with the modulation scheme used. The available modulation and coding schemes both in the downlink and uplink are QPSK, 16QAM and 64QAM for LTE. Then, the frequency domain modulated inputs are transformed into the time domain signal after the IFFT operation. As the last step, a CP is added and digital to analog conversion is performed and the signal is given to the transmission channel. The same stages are executed at the receiver part in reverse order.

Orthogonal Frequency Division Multiple Access (OFDMA) is the multiple access technique that is based on the OFDM transmission scheme. It allows the access of multiple users to the available bandwidth. It can be also regarded as a combination of time and frequency domain multiple access in which each user is assigned a time-frequency resource.

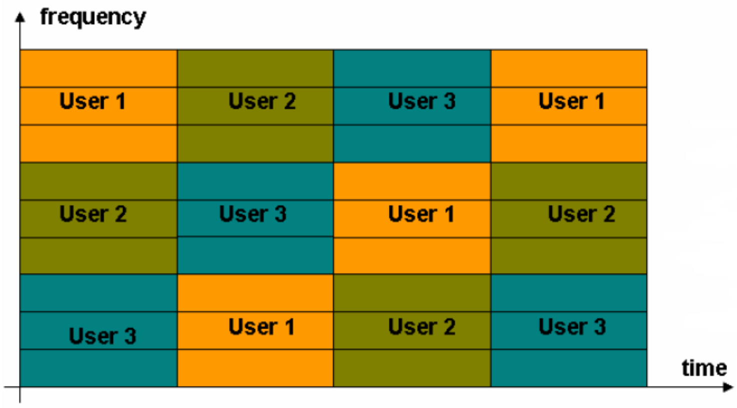

Figure 2-9 OFDMA time-frequency representation

In pure OFDM systems, only a single user can transmit on all of the subcarriers at any given time, and time division or frequency division multiple access is employed to support multiple users. The major drawback of this static multiple access scheme is the fact that frequency and multiuser diversity are not being utilized. On the other hand, OFDMA allows multiple users to transmit simultaneously on the different subcarriers per OFDM symbol. Since the probability that all users experience a deep fade in a particular subcarrier is very low, it can be guaranteed that subcarriers are assigned to the users which experience good channel gain on them. [5]

Single-Carrier Frequency Division Multiple Access (SC-FDMA), as previously mentioned, is the selected uplink transmission scheme for the LTE due to its low PAPR compared to OFDMA. The major disadvantage of multicarrier modulation, the PAPR, is defined as the ratio between the peak and average value of the transmitted signals. The peak values of some of the transmitted signals could be much higher than the typical values which lead to a requirement for implementing linear circuits within a large dynamic range. Otherwise, the signal clipping at high levels will produce a distortion of the transmitted signal and out-of-band radiation.

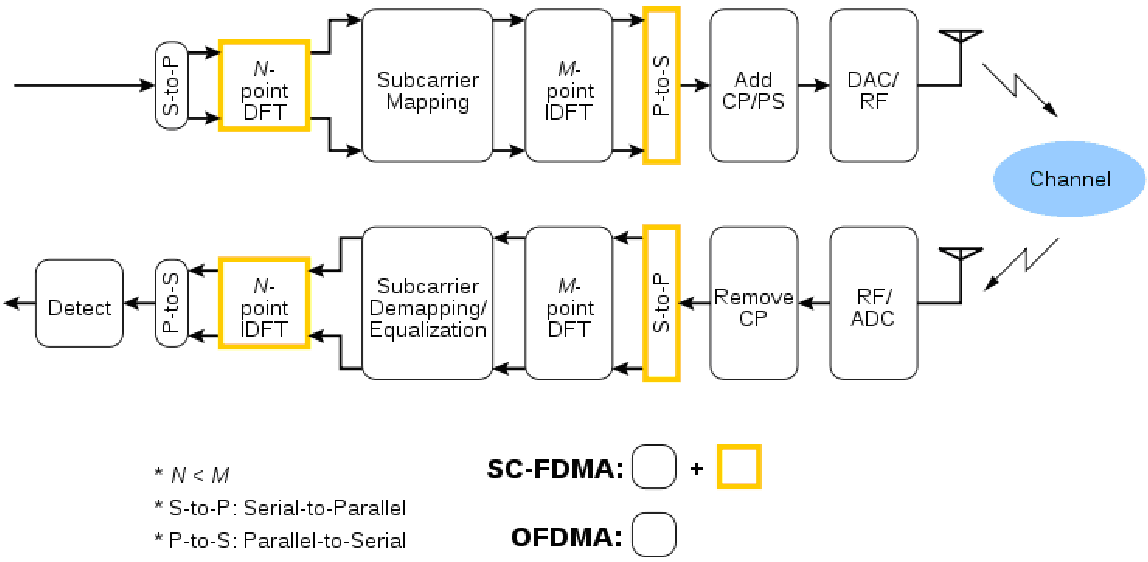

Figure 2-10 SC-FDMA and OFDMA Tx-Rx structure [10]

Moreover, SC-FDMA can be also considered as a Discrete Fourier Transform (DFT) - spread OFDM scheme which firstly applies an N-size DFT to a block of N modulation symbols. The modulation symbols which are generated with QPSK, 16QAM or 64QAM as E-UTRAN modulation schemes are transformed into the frequency domain by the DFT. The results are mapped onto the available subcarriers. An M point IFFT in which M>N is then executed as in OFDM, followed by the parallel to serial conversion and the addition of the cyclic prefix.

As given in Figure 2-10, the main difference between the OFDMA and SC-FDMA is the DFT processing before the symbol to subcarrier mapping. In a SC-FDMA signal, each subcarrier has the information of all transmitted modulation symbols due to the fact that DFT-spread input data stream is mapped to the available subcarriers. In contrast to this, each subcarrier of an OFDMA signal only carries information related to specific modulation symbols [8].

2.3.2 LTE uplink transmission

2.3.2.1 Frame structure and resource grid

The agreed uplink transmission scheme SC-FDMA for the 3GPP LTE is similar to the downlink. The radio frame structure used for both uplink and downlink transmissions is the same. Two frame structure types are defined in E-UTRAN, one for FDD mode and the other is for TDD mode in [9].

Frame structure type 1

The frame structure type 1 is applicable to both full duplex and half duplex FDD. Each radio frame is 10ms long and consists of twenty 0.5ms equally length slots, numbered from 0 to 19 and each subframe consists of 2 slots.

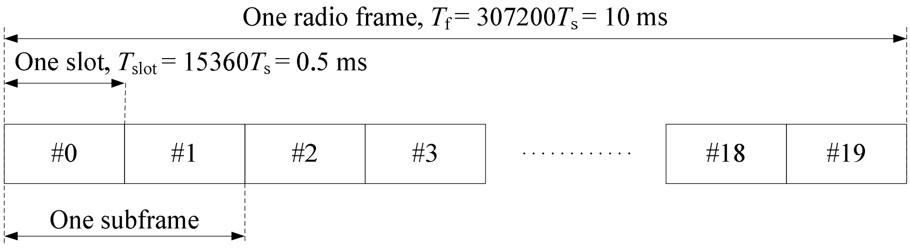

Figure 2-11 Frame structure type 1

For the FDD, 10 subframes are available for downlink transmission and 10 subframes are available for uplink transmission in each 10 ms interval. The uplink and downlink transmissions are separated in the frequency domain. In half-duplex FDD operation, the UE cannot transmit and receive at the same time while there are no such restrictions in full-duplex FDD.

Frame structure type 2

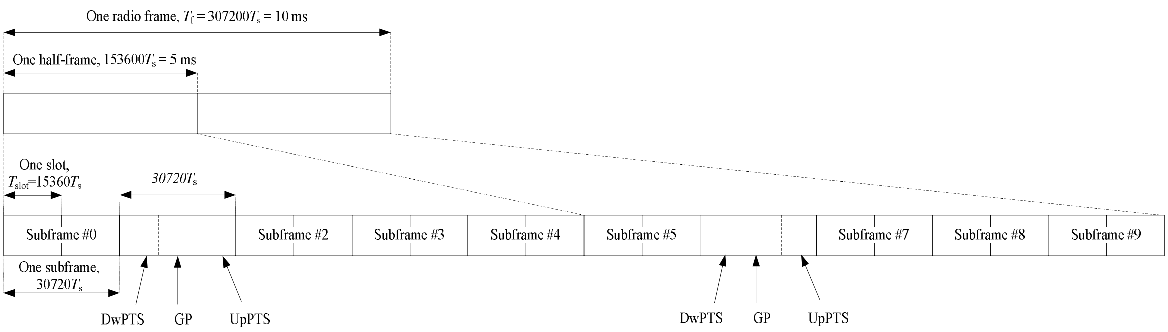

Figure 2-12 Frame structure type 2

The frame structure type 2 is applicable only in TDD and is provided for compatibility with legacy UTRA TDD systems.

Each radio frame consists of two equally sized half-frames. Both half-frames consist of eight 0.5ms slots and in addition there are special fields called Downlink Pilot Time Slot (DwPTS), Guard Period (GP) and Uplink Pilot Time Slot (UpPTS). The DwPTS is used for downlink synchronization and initial cell search. The GP determines the maximum cell size and it ensures that a UE transmitting the UpPTS does not disturb the reception of the DwPTS for other close-by UE. The UpPTS is used by the eNodeB to determine the received power level and received timing from the UE [30].

Subframes 0 and 5 and DwPTS are always reserved for downlink transmission. The first switching point between uplink and downlink is allowed at GP.

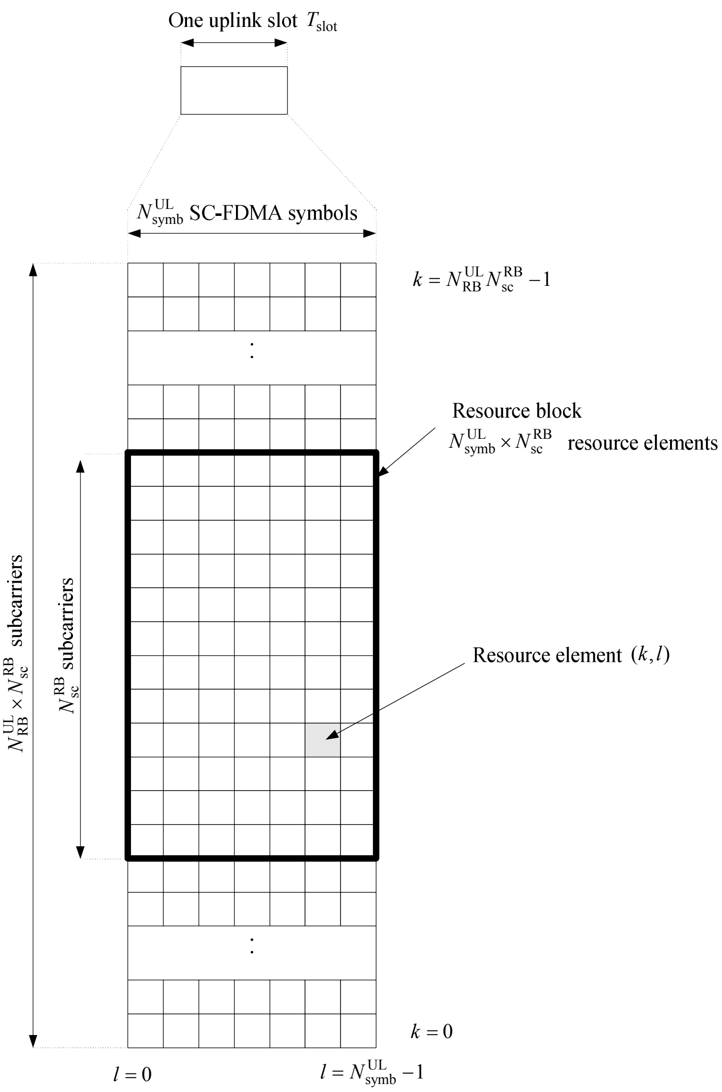

Figure 2-13 Uplink resource grid

As shown in Figure 2-13, the transmitted signal in each slot is described by a resource grid of $N_{RB}^{UL} N_{sc}^{RB}$ subcarriers and N_{symb}^{UL} SC-FDMA symbols.

Each element in the resource grid is called a resource element, and a Physical Resource Block (PRB) is defined as N_{symb}^{UL} consecutive SC-FDMA symbols in the time domain and N_{sc}^{RB} consecutive subcarriers in the frequency domain.

A physical resource block in the uplink thus consists of $N_{symb}^{UL} \times N_{sc}^{RB}$ resource elements, corresponding to one slot in the time domain and 180 kHz in the frequency domain which is 12 evenly spaced 15 kHz subcarriers.

The number of SC-FDMA symbols in a slot (N_{symb}^{UL}) depending on the cyclic prefix is shown in Table 2-1.

Cyclic Prefix	N_{sc}^{RB}	N_{symb}^{UL}	N_{symb}^{UL}
Normal cyclic prefix	12	7	9
Extended cyclic prefix	12	6	8

Table 2-1 Resource block parameters

Detailed transmission parameters for the FDD mode are given in Appendix A.

2.3.2.2 Uplink data transmission and channels

Data is allocated to the UEs in terms of PRBs, meaning that one UE can be allocated to the permitted integer multiples of one PRB in the frequency domain. However, not all the integers are permitted to be used so as to simplify the DFT design in the uplink unlike in the downlink. The scheduling decision can be modified at every Transmission Time Interval (TTI) of 1ms in the time domain.

The user data is carried on the Physical Uplink Shared Channel (PUSCH) and the control information is carried on the Physical Uplink Control Channel (PUCCH). The PUCCH is never transmitted simultaneously with the PUSCH from the same UE and it is transmitted on a reserved frequency region in the uplink. One other channel which is called the Physical Uplink Random Access Channel (PRACH) is used for carrying the random access information exchanges.

2.3.2.3 Uplink reference signals

The reference signals in the uplink are used for two different aims:

- channel estimation at eNodeB receivers in order to demodulate data and control channels
- granting channel quality information for the scheduling decisions at eNodeBs which is known as channel sounding

The generation of reference signals is performed with specific Zadoff-Chu sequence types and they are inserted within the fourth block of each uplink slot.

2.3.2.4 Physical layer procedures in uplink LTE

Random access

The random access is used to transfer information from a mobile to the network that is for initial access to the connection setup or for location area updates. There are two defined random access procedures by 3GPP, either contention based or non-contention based. The uplink random access preamble occupies a bandwidth of six resource blocks. The random access preamble includes a sequence with length $\boldsymbol{T_{SEQ}}$ and a cyclic prefix with length $\boldsymbol{T_{CP}}$.

Uplink scheduling

The eNodeB performs the uplink scheduling by assigning certain time/frequency resources to the UEs and informs the UEs about the transmission formats to use. The Physical Downlink Control Channel (PDCCH) transfers the scheduling grants to the UEs. The scheduling decisions might be based on uplink channel quality measurements, QoS parameters, UE buffer status, UE capabilities as well as other variables.

Uplink link adaptation

Transmission power control, Adaptive Modulation and Coding (AMC) and adaptive transmission bandwidth can be used to maintain the link adaptation in the uplink.

Uplink timing advance (control)

The timing advance is a negative offset which is between the start of a received downlink subframe and a transmitted uplink subframe at the UE. It is meant to control the timing of signals received at the eNodeB.

Hybrid ARQ

The Hybrid Automatic Repeat Request (HARQ) protocol which was already implemented in HSUPA will be also implemented in LTE. It is used for the retransmission of the incorrectly received data packets via the request of the eNodeB. The ACK/NACK information in the downlink is sent on a Physical Hybrid ARQ Indicator Channel (PHICH).

Multiple Input Multiple Output (MIMO) systems to achieve higher throughputs and spectral efficiency, LTE Multimedia Broadcast Multicast Services (MBMS) and detailed LTE protocol structures are excluded from consideration as they all lie beyond the scope of this present work.

3 LTE ADVANCED AND RELAYING

This chapter introduces the *3GPP LTE Advanced* standardization and discusses one of its proposed catalysts, the *Relaying* concept for achieving the requirements of the novel standard.

3.1 LTE Advanced (LTE-A)

The 3GPP LTE standardization has developed to a mature level by early 2009. The latest set of standards with Release 8 are expected to be ready before the end of 2009 and they will combine the completion of 3GPP Release 7 HSPA+ features, voice over HSPA, Common IP Multimedia Subsystem (IMS) and LTE standards. LTE networks are anticipated to be deployed from 2010 onwards as a natural evolution of GSM and UMTS [14].

Moreover, ITU has already approved IMT Advanced which relates to 4G as an upgrade of 3G networks. The mobile communication industry and standardization groups were invited by ITU to submit their candidate radio interface technologies that follow the requirements of IMT Advanced. LTE Advanced (LTE-A) is the new standardization proposal of 3GPP which corresponds to IMT Advanced. The concept was first agreed in April 2008 at the IMT advanced workshop in China as a major enhancement of 3G LTE. The LTE-A which is aimed to be processed initially in Release 10 fulfills the requirements of IMT Advanced addressed by ITU. The first set of requirements on the 3GPP LTE-A has been described in a technical report (TR 36.913) published in June 2008. The following section introduces the requirements that are presented in this technical report.

3.1.1 Requirements of LTE Advanced

The requirements for LTE Advanced standardization is listed as follows:

General requirements

LTE Advanced shall be an evolution of LTE by satisfying all requirements and targets of 3GPP TR25.913 (Requirements for E-UTRA and E-UTRAN), supporting existing LTE terminals, and working in existing LTE part of networks and providing higher performance compared to the expected requirements of IMT Advanced in ITU-R.

Capabilities and system performance requirements

Some of the capabilities and the system performance targets of 3GPP LTE and approved 3GPP requirements for LTE Advanced are compared in Table 3-1.

Standards	**LTE**	**LTE Advanced**
Peak data rates	100 Mbps in DL 50 Mbps in UL	1 Gbps in DL 500 Mbps in UL
Bandwidth	up to 20 MHz	up to 100 MHz
User plane latency	5 ms	Improved compared to LTE
Control plane latency	50/100 ms	10/50 ms
Peak spectrum efficiency	5 bps/Hz in DL 2.5 bps/Hz in UL	30 bps/Hz in DL 15 bps/Hz in UL

Table 3-1 LTE targets and 3GPP requirements on LTE Advanced

It should be noted that the given peak spectrum efficiency targets for LTE-A are not exactly translated from peak data rates considering a 100 MHz bandwidth.

Moreover, the average spectrum efficiency (aggregate throughput of all users) and cell edge spectrum efficiency (5%ile user throughput) targets with four different scenarios and several antenna configurations are enhanced compared to ITU requirements and LTE Release 8. More information can be obtained from [15]. Mobility support shall be maintained up to 350km/h (or even up to 500km/h depending on the frequency band). VoIP capacity should be also improved compared to LTE Release 8. Coverage requirements of LTE-A shall be similar to LTE requirements [1].

Deployment-related requirements

Release 8 E-UTRA terminal can work in an Advanced E-UTRAN and an Advanced E-UTRA terminal can work in a Release 8 E-UTRAN. New frequency bands are identified for Advanced E-UTRA. Advanced E-UTRA may operate in wider spectrum allocations than Release 8 E-UTRA. Network sharing and handovers with legacy radio access technologies shall be supported.

Cost-related requirements

The essential points in cost reductions are low cost infrastructure deployment and terminals for LTE Advanced. Power efficiency in the infrastructure and in the terminals will be a necessity. Backhauling is aimed to minimize cost per bit.

Besides the aforementioned points, radio resource management, complexity as well as the service-related requirements of LTE Release 8 shall be applicable and improved for the LTE Advanced standardization.

3.1.2 Standardization and proposals

The standardization of LTE Advanced is expected to be included in 3GPP's Release 10 timeframe. Deployment of LTE Advanced networks is anticipated to be roughly sometime between 2012 and 2015 as an upgrade to LTE.

The proposal, evaluation, consensus and the finally specification process of LTE Advanced will be continuing in the near future. Furthermore, the proposal phase has already started and many mobile communication companies are contributing to the progress.

The categorization of the proposals from [16] to achieve the targets and requirements of the LTE Advanced standardization presented at the IMT Advanced workshop in April 2008 will be listed as the following:

- relaying
- UE dual Tx antenna solutions for SU-MIMO and diversity MIMO
- scalable system bandwidth exceeding 20 MHz, potentially up to 100 MHz
- local area optimization of air interface
- nomadic / local area network and mobility solutions
- flexible spectrum usage
- automatic and autonomous network configuration and operation

3.1.3 Relaying proposal for LTE-A

Most of the proposals for maintaining the LTE-A requirements and targets from different mobile communication companies are parallel to each other. However, there remain a few differences and investigation of the techniques and components is still an ongoing process. The relaying concept, however, is proposed by all of the mobile technology companies. The reasons to introduce this relaying concept in the LTE-A networks are the following:

The requirements have been addressed by IMT: improved cell edge capacity, low OPEX deployment and reduced backhaul cost and enhanced network topology can be granted with the relaying concept which:

- enhances coverage for medium and high data rate services
- enhances cell throughput (in particular contribution from cell edges)
- increases capacity in a cost efficient way without new macro sites plus backhauls [16]

Nevertheless, the kind of relay nodes to be used in the system is still under investigation. Detailed information of the relaying concept and features of the relay nodes will be examined in the next section.

3.2 Relaying

The novel future broadband wireless communication networks will be introduced by the LTE-A release. Relay enhanced networks are one of the proposals to meet the requirements of the LTE-A. This section of the report presents a general introduction to the relaying rationale.

3.2.1 The need for relaying

The envisioned high data rate transmission with the upcoming future wireless communication networks arouses curiosity to make investigations for upgrades to the current networks. As mentioned in the previous section about the targets of the new LTE-A, the relaying concept is one crucial topic to investigate.

The frequency spectrum bands used for the future communication networks are operating on 2 GHz and higher carrier frequencies where the radio transmission is subjected to severe path loss and channel fading. An increased transmission rate, therefore, requires higher transmit powers to maintain the same coverage, whereas the transmission powers are already limited. Furthermore, propagation conditions especially in urban areas restrict the radio coverage.

A solution to these limitations would be to increase the transmit power levels which in turn leads to higher interference within the system. Another option would be to increase the density of base stations which then results in higher deployment and maintenance costs since the number of subscribers may not grow proportionally. However, high data rates would still be possible only for the users close to the base stations with this kind of solution.

A more robust and promising technique to satisfy the high throughput and coverage requirements of future networks would be the introduction of the relay nodes into the network infrastructure.

3.2.2 Benefits of relaying

- The main improvements that can be achieved with relaying are increased capacity and extended coverage in an efficient way. Relay based deployment can also provide fair capacity distribution in the cell area [11].

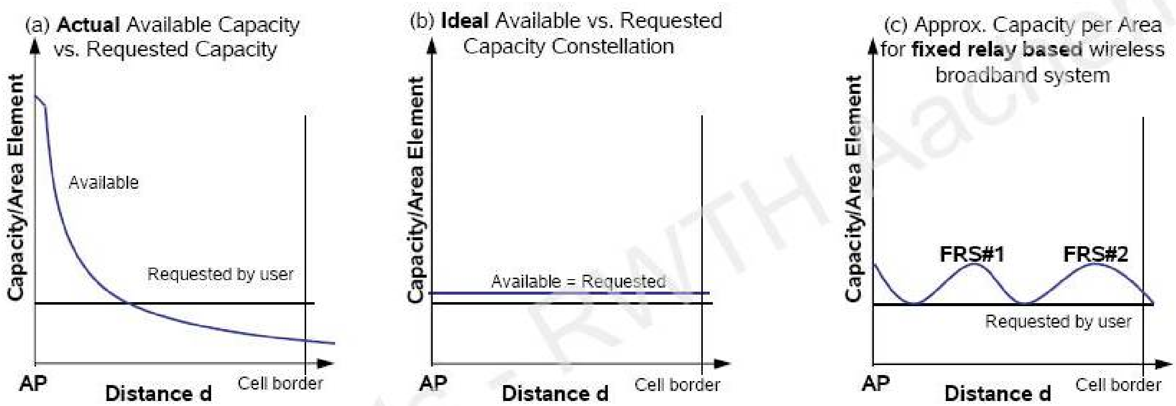

Figure 3-1 Capacity vs. user demand [11]

- The capacity can be distributed over the cell coverage area close to the ideal case by means of relay based deployment, which can be observed in Figure 3-1.
- Relay nodes do not need a wired connection to the system backhaul. They just store the received data and forward it to the destination. This substantially lowers the cost of infrastructure and operation.
- Relay nodes are not required to be placed as high as base stations; they can be located below rooftop level such as on top of lampposts, also decreasing the operational expenses such as tower leasing and the maintenance costs for the service provider [12].
- Users near the relay nodes will be consequently served by them, thus higher data rates can be maintained for these users since the pathloss will be respectively

smaller.

- Similarly, users near the cell border experience low SINR and then low throughput in a base-station-only deployment. Relays can be the solution in this case as well.
- From the operator point of view, the benefits of relaying can be seen as simplified and cost efficient deployment by means of reduced OPEX and CAPEX.

3.2.3 Drawbacks of relaying

- Relays introduce extra delay and overhead in the system.
- Resource partitioning and interference management become important issues; in-band relays consumes radio resources and out-of-band relays need multiple transceivers. [11]
- Deployment is challenging. The decisions for relay based deployment might vary for different application scenarios, such as urban or rural areas.
- Design of additional set of signaling protocols is needed depending on the relay node types.
- An increased number of hops introduce more complexity and overhead in the system. The amount of multi hops should be decided appropriately.

3.3 Classification of relays

Relays can be referred to as enhanced repeaters. The frame structure and functional split of Layer 1, Layer 2 and Layer 3 relays are still under discussion in the literature [13]. The relay nodes working on different layers will provide dissimilar capacity and coverage results for each different system scenario.

Classification can be also made under amplify-and-forward (AF) and decode-and-forward (DF) categories where Layer 1 relay nodes are considered as AF while Layer 2 and Layer 3 relay nodes are considered as DF. In this report, the AF and DF relays are evaluated. The following section will provide a further insight into the concept.

3.3.1 Amplify-and-forward (AF) relaying vs. Decode-and-forward (DF) relaying

An *amplify-and-forward* relay node acts as an analog repeater and basically amplifies and forwards the received signal from the source to the destination in the physical layer. However, the AF relay node cannot distinguish the desired signal from interference and noise; therefore, it also amplifies the noise and interference. This does not help to improve the network capacity. Yet, coverage extension would be performed by the conventional AF relay nodes especially in noise limited scenarios. The main advantage of the AF relays over the DF relays is less delay in the transmission.

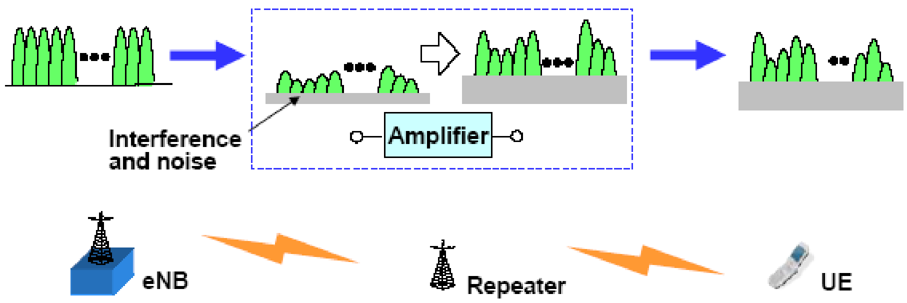

Figure 3-2 Amplify-and-forward relaying [22]

On the other hand, a *decode-and-forward* relay node, that is smarter than an AF one, decodes and re-encodes the received signal from the source and then forwards it to the destination in Layer 2. Hence, no interference/noise amplification appears in the network due to the relaying which then leads to improved capacity. Since the encoding is performed again, Adaptive Modulation and Coding (AMC) can be used in different hops. Radio Resource Management (RRM) methods can be also applicable for the DF relay nodes to advance both the capacity and coverage.

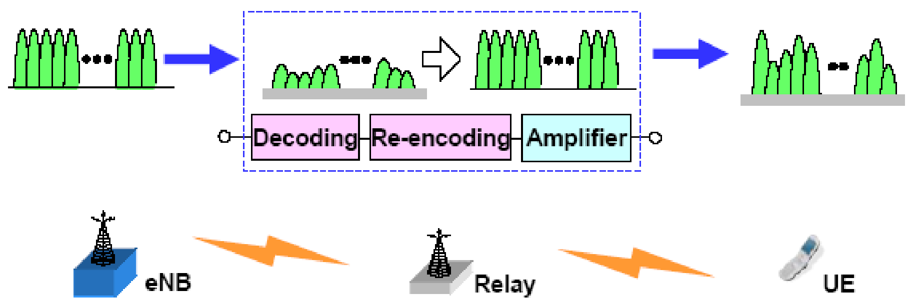

Figure 3-3 Decode-and-forward relaying [22]

Some of the advantages and disadvantages of the AF and the DF relay nodes are listed in Table 3-2.

Relay Type	Advantages	Disadvantages
AF	▪ coverage improvement ▪ low cost	▪ noise amplification ▪ RF isolation issues ▪ no need in PHY/MAC change ▪ no power control
DF	▪ no noise amplification ▪ throughput and coverage improvement ▪ can support beamforming ▪ can support power control and AMC and RRM methods	▪ changes to PHY/MAC ▪ latency issues at UE

Table 3-2 Comparison of AF and DF relaying

3.4 Heterogeneous cells in LTE-A

The latest 3GPP contribution, which presents the evaluation methodology for the LTE-A studies, includes heterogeneous cell deployment scenarios [18]. This consists of deployments where lower powered nodes that are referred as the relay nodes in this work, are placed in a macro cell layout.

3.4.1 Heterogeneous cell deployment

Unlike ad-hoc networks, fixed relay nodes (RN) are placed at pre-defined positions in the LTE concept. This type of deployment was already extensively researched and examined under the Wireless World Initiative New Radio (WINNER) project [20]. Fixed relays for coverage and capacity enhancement were also standardized by IEEE802.16, task group “j” with the Mobile Multihop Relays (MMR) term [21].

A simple scenario of a multi hop deployment is shown in Figure 3-4 in which we consider a two-hop cell. This type of scenario is most attractive from a practical perspective due to the fact that the complexity in the system increases with more hops [17].

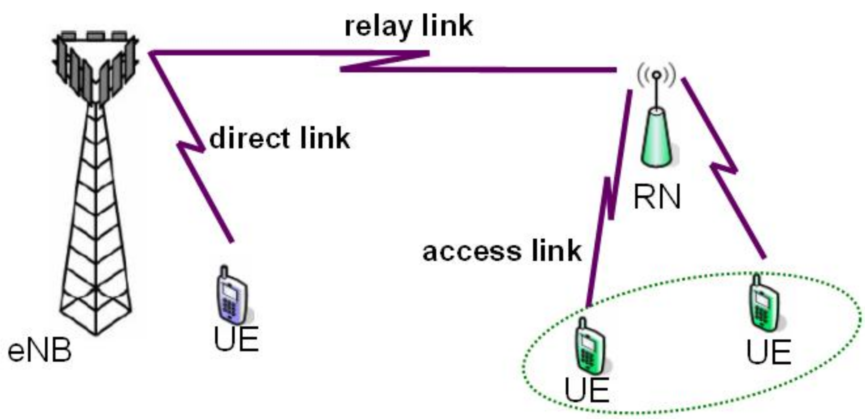

Figure 3-4 Multi hop deployment (two-hop)

In the deployment scenario, *direct link* refers to the link between the eNB and UE, *relay link* is used between the eNB and RN, and *access link* maintains the link between the RN and UE.

This type of scenario will be applied and studied throughout this work.

4 UPLINK POWER CONTROL IN LTE

This chapter discusses *power control* rationale. The various types of power control schemes and their application in different baseline technologies such as GSM, WCDMA and LTE are overviewed. The uplink fractional power control scheme of LTE is described and, finally, its performance evaluation is examined.

4.1 Power control rationale

> *"Power control (PC), broadly speaking, is the intelligent selection of transmit power in a communication system to achieve good performance within the system. The notion of "good performance" can depend on context and may include optimizing metrics such as link data rate, network capacity, geographic coverage and range, and life of the network and network devices." [23]*

Transmission power is a key factor in wireless networks dimensioning. The power control represents settings of the power levels for base stations (BS) in downlink (DL) and mobile stations (MS) in uplink (UL) transmission in cellular wireless networks. The main reasons to execute the transmission power control in a cellular wireless network can be listed as follows:

- to improve system capacity, coverage and user data rate
- to mitigate intra-cell and inter-cell interferences
- to reduce power consumption and conserve mobile station battery

It is necessary to determine appropriate transmission power levels for a proper power control scheme in order to achieve these objectives.

Wireless channels are subject to variations. For this reason, power control schemes are divided into two parts, according to which variations of a wireless channel requires adjustment:

- *Slow power control* is used to compensate for the slow channel variations such as distance dependent pathloss, shadow fading and antenna losses.
- *Fast power control* is used to compensate for the fast channel variations such as fast fading.

Moreover, two more different distinctions in power control schemes are also considered according to the information properties which are transmitted to a mobile station to set its power level:

- *Open loop power control* (OLPC) where the power is set in the mobile station by using the received power control message from the base station. No feedback is sent to the e-NB.
- *Closed loop power control* (CLPC) where the mobile station also sends feedback to the base station which is then used to correct transmission power in the mobile station.

It is observed that a fast closed loop power control scheme would provide optimum interference mitigation and compensate for channel variations with a rapid mechanism but it, however, also requires extra signaling overhead. From the other perspective, it is also observed that a slow open loop power control, although simple and having a low signaling overhead, would be insufficient to compensate for channel variations as efficiently as a closed-loop scheme. Selection of a power control scheme to be applied in a wireless network varies according to the different baseline technologies such as WDCMA or OFDMA.

4.2 Power control in GSM, UMTS and HSPA

In traditional GSM networks, a slow power control was implemented and mobile stations are separated into five different classes according to their peak transmit power levels as 20, 8, 5, 2 and 0.8 Watts respectively. Eight different classes are also assigned for base stations according to their maximum power levels: these are 320, 160, 80, 40, 20, 10, 5 and 2.5 Watts, respectively. Mobile stations and base stations both operate at the lowest power level which still maintains an acceptable link quality. Power levels can be ascended or descended in steps of 2 dB from the peak power down to a minimum of 13 dBm (20 milliwatts). Mobile stations and base stations measure the signal quality based on the Bit Error Rate (BER) and report it to the Base Station Controller (BSC) which is responsible for changing the power level when necessary.

In WCDMA, fast closed loop power control is applied both in downlink and uplink with 1.5 kHz frequency. This is unlike GSM where only slow power control is employed with an approximate frequency of 2 Hz [2]. Fast power control is one of the most important aspects in interference limited WCDMA systems, particularly in uplink. Signals of different mobile stations are transmitted simultaneously within the same frequency band in CDMA systems. Scrambling codes that are used for user separation in uplink are not orthogonal to each other. The signal from a user situated closer to the base station may block (non decodable signal at the receiver) another signal from a user further away from the base station, and in the worst case, a single over-powered mobile station could even block whole cell. This phenomenon is called the *near-far-effect*. Power control aims to remedy this situation by equalizing the received powers of all users at the receiver to maintain a proper decoding. In downlink transmission, the near-far-effect problem does not exist due to one-to-many scenarios. Orthogonal spreading codes separate users within a cell to separate the users. However, power control is still applied to mitigate inter-cell interference.

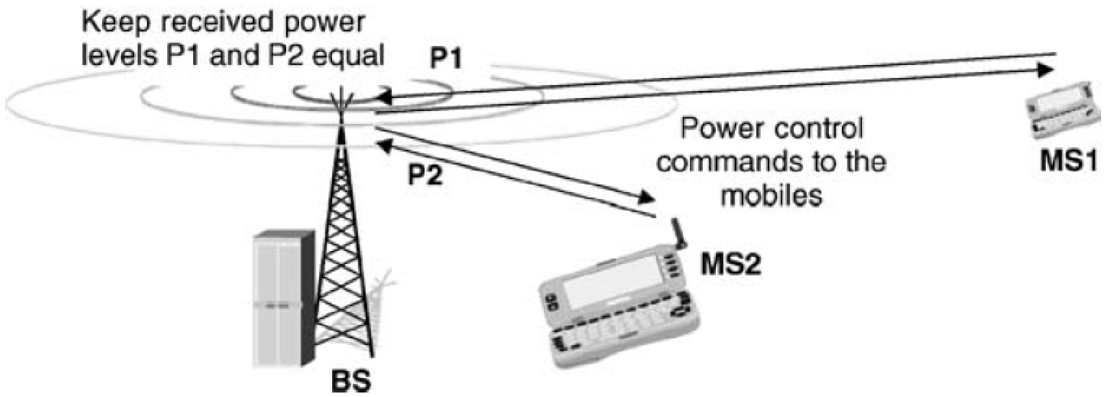

Figure 4-1 Closed loop power control in CDMA [2]

Open loop power control is basically applied by the base station at the initial state of transmission to estimate the required transmission power of a mobile station for a target SINR to ensure a desirable error rate. Firstly, the SINR target value is broadcasted to the mobile station via the broadcast channel. The mobile station subsequently estimates the distance based pathloss considering also the shadowing to the base station based on the received signal power on the common pilot channel which is sent at a known power level. Finally, the mobile station adjusts it's transmit power to achieve the SINR target by taking also the estimated broadcast interference and noise levels into account.

In closed loop power control, the base station estimates the SINR of the received signal and compares it with the target SINR value. A power control command "UP" (increase transmission power) is sent to a mobile station when the SINR of the received signal is lower than the target SINR value; otherwise the “DOWN” command is delivered to decrease the transmission power of mobile station. The mobile station subsequently adjusts its power according to the predefined step sizes. The target SINR is decided by an outer loop power control which updates the desired target SINR based on the frame error rate estimation at the base station. Consequently, the closed loop power control update rates are frequently compared to the outer loop power control update rates.

In HSDPA, rate control is preferred as a link adaptation procedure instead of power control. Especially, in case of packet data traffic, a constant data rate is not a critical requirement. From the user point of view, it is desirable to have as high a data rate as possible.

Rate control maintains the SINR at the desired level, not by adjusting power levels but rather by adjusting the data rate in the system. As a result, power amplifiers are used more efficiently.

Figure 4-2 illustrates how power control and rate control work in a fading channel.

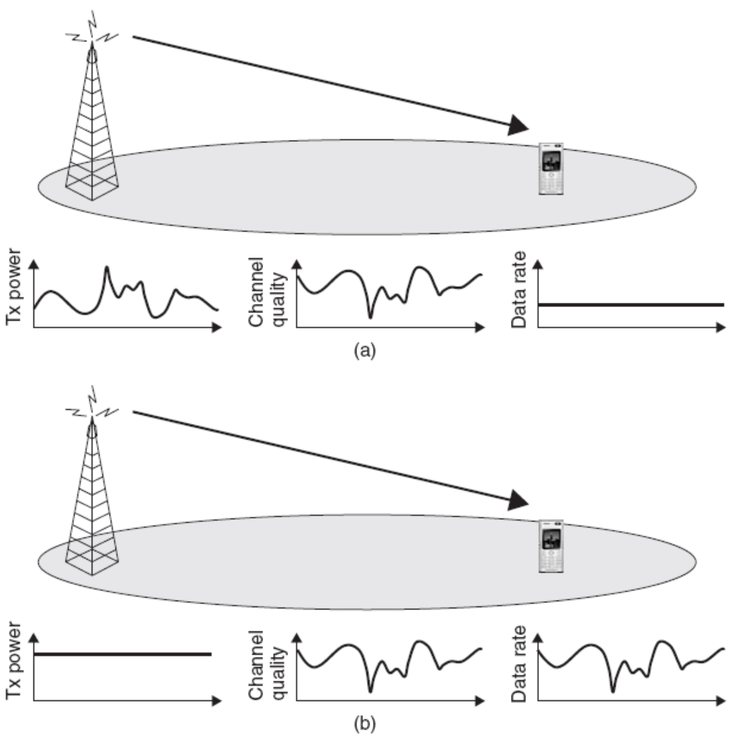

Figure 4-2 a) Power control and b) Rate control [3]

The rate control is executed by the configuration of the modulation scheme and channel coding rate according to the channel quality. In fair channel qualities, a higher order modulation like 16QAM or 64QAM with a high code rate is appropriate. Rate control for link adaptation is, therefore, also referred to as Adaptive Modulation and Coding (AMC).

In HSDPA, other aspects like channel dependent scheduling and HARQ additional to AMC form a more efficient combination compared to power control alone. Hence, fast closed loop power control is no longer applied in HSDPA systems. The open loop power control, however, does in fact remain.

In HSUPA, similar to WCDMA, transmission in the uplink is non-orthogonal and still subject to interference between uplink transmissions within the same cell. Therefore, fast power control is essential to deal with the near-far-effect problem in the uplink. A scheduler becomes more important to control the data rates in HSUPA. An increase in transmission power of a user results in higher data rates. However, it also gives rise to interference for the other users due to its non-orthogonal nature. The interference level represents the reliability of the uplink transmission. Consequently, the uplink scheduler in HSUPA grants as high data rates as possible for the users without exceeding the maximum tolerable interference level in the system.

4.3 Power control in LTE uplink

The LTE uplink multiple access scheme SC-FDMA is an orthogonal access technique that avoids the intra-cell interference and the near-far-effect problem typical for CDMA based systems like WCDMA and HSPA. Therefore, fast power control to keep track of fast fading is not required for the LTE uplink. Slow power control with channel dependent scheduling, which is accompanied by HARQ, will be sufficient to cope with fading in the LTE uplink transmission.

However, the system remains sensitive to inter-cell interference as there is no orthogonality between the signals of neighboring cells. As a result of this, a slow open loop power control becomes vital to maintain the required SINR while at the same time controlling the interference caused to neighboring cells.

Conventional slow, open loop power control schemes compensate for pathloss and shadowing while trying to maintain the same SINR at the receiver for all users in the system. There is a problem when using this scheme to control the inter-cell interference since it fails to consider the fact that users located near the cell center do not contribute to the inter-cell interference as much as the users located near the cell-edge. 3GPP has approved the PC formula that takes into account the mentioned problem by including the parameter α in the formula which basically allows for fractional power control. This permits users that have low pathloss to operate at a higher SINR in order to obtain high spectral efficiency.

In LTE, uplink power control defines the transmit power of the different uplink physical channels such as the Physical Uplink Shared Channel (PUSCH) and the Physical Uplink Control Channel (PUCCH). The 3GPP has already standardized the PC formula for these channels. Since data is transmitted over PUSCH, this work will consider the approved PUSCH power control formula given in Equation (1). The transmitting power is set at the User Equipment (UE) using control commands and parameters received from the eNodeB according to the given formula:

$$\boldsymbol{P} = \mathbf{min}\{\boldsymbol{P}_{\mathbf{max}}, \boldsymbol{P}_0 + 10\,\mathbf{log}_{10}\,\boldsymbol{M} + \boldsymbol{\alpha L} + \Delta_{\boldsymbol{TF}}(\boldsymbol{i}) + \boldsymbol{f}(\boldsymbol{i})\} \quad \text{[dBm]} \qquad (1)$$

where:

- $\boldsymbol{P}_{\mathbf{max}}$: maximum allowed UE transmit power
- $\boldsymbol{M}$: number of allocated Physical Resource Blocks (PRBs) to a user
- $\boldsymbol{P}_0$: power contained in one PRB which has cell specific and UE specific parts (is used to control the SINR target)
- α : a cell specific pathloss compensation factor
- $\boldsymbol{L}$: the downlink pathloss estimated at the UE based on the transmit power of the reference signal
- $\Delta_{\boldsymbol{TF}}(\boldsymbol{i})$: MCS dependent offset (UE specific)
- $\boldsymbol{f}(\boldsymbol{i})$: is a function which has closed loop corrections values (UE specific)

The physical layer specifications and detailed parameter features of uplink power control can be found in the latest 3GPP technical report [28].

In this work, the performance of only open loop power control will be considered; therefore, it is sufficient to take the open loop parameters and the pathloss information into account to make a simplified evaluation. $\boldsymbol{P}_0$ and α are the open loop terms in the formula, which are transmitted to the UEs as a broadcast by the eNBs. The closed loop terms $\Delta_{\boldsymbol{TF}}(\boldsymbol{i})$ and $\boldsymbol{f}(\boldsymbol{i})$ are used after the initial transmit power setup of the open loop terms.

These parameters can be signaled to UEs and then, UEs send feedback to the eNBs to adjust the transmit power. As it can be observed, the initial step is to define the transmit power for UEs by means of open loop terms.

It is important to discuss what quantity of power should be controlled in LTE. In contrast to UMTS systems in which the whole bandwidth is occupied by the mobile station, in LTE uplink resources are assigned as a fraction of the whole transmission bandwidth. Therefore, from the PC point of view in LTE, it is necessary to define the transmitting power of a PRB. This means that it is more appropriate to assign the mobile station's transmit Power Spectral Density (PSD) instead of assigning the total transmit power. In LTE, it is assumed that the transmit PSD will be the same over all the physical resource blocks and one PRB has a bandwidth of 180 kHz [24].

The OLPC procedure in LTE uplink resembles WDCMA. The UE receives the SINR target from the eNB and estimates the pathloss and shadow fading by long term measurements of the received signal power of the common pilot channel which is sent at a known power level. The eNB informs the UE about the average uplink interference level per PRB through downlink broadcast channels or the scheduling grant. The uplink interference is composed of the inter-cell interference, which can be described as $\boldsymbol{IoT}$ and thermal noise $\boldsymbol{N}$. Then, UE adjusts its transmit power to achieve the target SINR.

The OLPC formula can be simplified by removing the closed loop terms as:

$$\boldsymbol{P} = \mathbf{min}\{\boldsymbol{P}_{\mathbf{max}}, \boldsymbol{P}_0 + 10\,\mathbf{log}_{10}\,\boldsymbol{M} + \boldsymbol{\alpha L}\} \text{ [dBm]} \qquad (2)$$

As can be seen from the formula, α defines the fraction of how much pathloss is compensated. 3GPP specifications define that α can take values in the range of [0, 1] with allowable values [0, 0.4, 0.5, 0.6, 0.7, 0.8, 0.9, 1]. This formula implies that PC defines the transmit power in one PRB and UE scales it to the transmission bandwidth by taking the number of assigned PRBs into account. As a result, we have constant power level for each PRB in the system. In other words, constant PSD is used over the whole transmission bandwidth. Therefore, it would be more appropriate and simpler to show transmit PSD per PRB in the formula by eliminating the logarithmic term. Finally, transmit PSD per PRB is given in Equation (3) as:

$$\boldsymbol{PSD} = \boldsymbol{P}_0 + \boldsymbol{\alpha L} \qquad \text{[dBm]} \qquad (3)$$

If the experienced SINR per PRB is defined as in the following:

$$\boldsymbol{SINR} = \boldsymbol{PSD} - \boldsymbol{L} - \boldsymbol{IoT} - \boldsymbol{N} \qquad [\text{dB}] \qquad (4)$$

where:

$\boldsymbol{IoT}$ is the interference over thermal and $\boldsymbol{N}$ is the thermal noise. The $\boldsymbol{IoT}$ describes the interference similar to the rise of thermal in CDMA systems, standing for the total received interference power divided by the thermal noise. Substituting Equation (3) in (4) the SINR experienced per PRB can be written as:

$$\boldsymbol{SINR} = \boldsymbol{P}_0 + (\alpha - 1)\boldsymbol{L} - \boldsymbol{IoT} - \boldsymbol{N} \qquad [\text{dB}] \qquad (5)$$

As can be observed from the formula, $\boldsymbol{P}_0$ and α are actually the parameters that are used to control the SINR target as well for the initial power settings.

Finally, the effects of the parameters $\boldsymbol{P}_0$ and α on the transmit PSD per PRB, SINR and throughput distribution can be examined and optimal values for different deployment scenarios, such as interference-limited or noise-limited, can be considered.

Prior to these investigations, the snapshot uplink simulator that is used in this thesis will be briefly described in the next section.

4.4 Snapshot uplink simulator

The system level simulator that is written in MATLAB and used in this work follows the latest proposal of the evaluation methodology for LTE-A studies given in [18].

4.4.1 Characteristics of the simulator

The main characteristics of the static snapshot UL simulator are listed as follows:

eNB deployment: regular on hexagonal grid (19 cells), 3 sectors/cell

Inter-site-distance (ISD): Macro1 (500m) or Macro3 (1732m)

UE deployment: desired number of users randomly generated (8 or 48)

RN deployment: regular at the cell borders (1, 2 or 3 tiers)

Transmit powers: different Tx powers for eNBs, RNs and UEs

Channel models: latest channel models for LTE-A evaluations are used. Shadowing and fast fading are not considered. Margins can be used to take into account shadowing and differences in the link budget (e.g. noise figure, cable loss, etc.)

Spatial processing: directional antennas at eNB and omni-directional antennas at RN

System bandwidth: 10 MHz (48 PRBs)

Carrier frequency: 2 GHz

Duplexing scheme: FDD/TDD (simulation window is one TTI)

Traffic model: uplink, full buffer

Packet scheduling: round robin (RR)

Power control: based on 3GPP formula both for users connected to eNB and RN

Throughput calculation: based on LTE hull curve approximation

4.4.2 Simulation parameters

Some of the main simulation parameters adopted from [19] are presented in Table 4-1.

PARAMETER	ASSUMPTIONS
System layout	19 cells & 3 sectors/cell &1, 2 or 3 tiers of RNs/sector
Carrier frequency	2 GHz
Propagation scenario	Macro1 (500m ISD) and Macro3 (1732 ISD)
Frequency planning	Reuse 1 (each eNB and RN UL transmission interferes with each other)
System bandwidth	10 MHz (48 PRBs for data)
Channel models	eNB-UE -> 3GPP TR 25.942 $\boldsymbol{L} = 128.1 + 37.6\,\mathbf{log}_{10}\,\boldsymbol{R}$ (R in km) eNB-RN -> 3GPP R1-084026 $\boldsymbol{L} = 124.5 + 37.6\,\mathbf{log}_{10}\,\boldsymbol{R}$ (R in km) RN-UE -> 3GPP R1-084026 $\boldsymbol{L} = 140.7 + 36.7\,\mathbf{log}_{10}\,\boldsymbol{R}$ (R in km)
Antenna pattern	$A(\theta) = -\mathbf{min}\left[12\left(\frac{\theta}{\theta_{3dB}}\right)^2, A_m\right]$ $A_m = 25\text{ dB}$, $\theta_{3dB} = 70^o$
UE transmit power	23 dBm
eNB transmit power	46 dBm
RN transmit power	30 dBm
Penetration loss	20 dB (only at direct and access links)

Extra margins	0 dB (no shadow fading and fast fading)
Traffic model	Uplink full buffer
UE scheduling	Round robin
User drop	48 users per Sector / 200 iterations
Simulation window	1 TTI

Table 4-1 Simulation parameters

A comprehensive simulator description including cellular network architecture, propagation models, system models and user and traffic models with some simulation assumptions and parameter settings is given in Appendix B.

4.5 Performance evaluation for fractional power control

The performance of LTE uplink fractional power control has been evaluated for Macro cell scenarios in previous works [25] and [26]. A modified uplink power control scheme which takes into account the pathloss differences between the mobile station's serving cell and the strongest neighboring cell has been investigated in [27]. In this section, an overview of the performance of fractional power control in eNB-only scenarios considering a Macro1 ISD 500m will be given. Subsequently, parameter configurations for Macro1 noise limited and Macro3 interference limited scenarios will be defined. The next steps will include the performance evaluation of the power control in relay enhanced cells as well as proposing new approaches for the optimization.

4.5.1 Parameter impacts on SINR distribution and interference

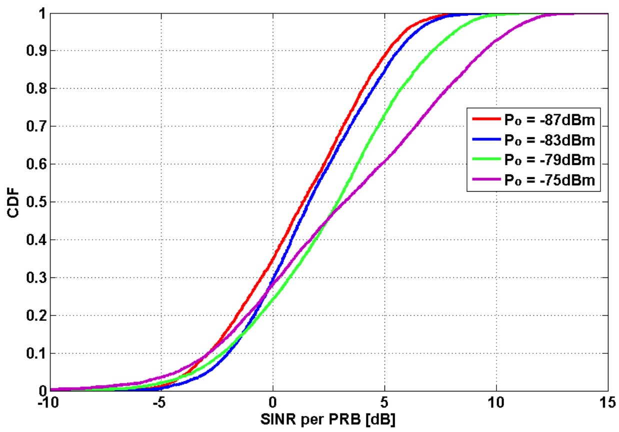

Figure 4-3 CDF of SINR per PRB as a function of different P_0 values

Figure 4-3 shows that a general SINR increase can be obtained with a higher $\boldsymbol{P}_0$ value when α is fixed (set as 1). Increasing $\boldsymbol{P}_0$ is not directly mapped into a considerably rise in SINR per PRB due to the fact that it also boosts all users powers, leading to a higher level of interference. Additionally, as can be observed from the 5 % ile profile in the plot, users near the cell-edge may experience a slightly lower SINR with an increasing $\boldsymbol{P}_0$ value after the amount of users transmitting with maximum power becomes corruptive.

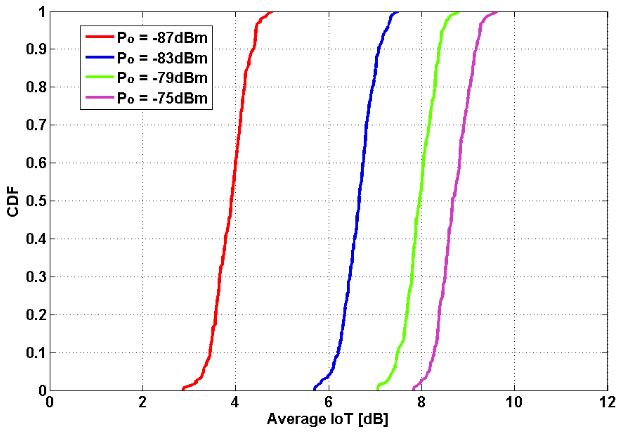

Figure 4-4 CDF of average IoT per PRB as a function of different $\boldsymbol{P}_0$ values

As can be seen from Figure 4-4, an increase in $\boldsymbol{P}_0$ is translated into an overall interference rise in the system. The interference rise in CDF curves is not proportional to each other even if the $\boldsymbol{P}_0$ intervals are the same (4 dB). This is due to the effects of inter-cell interference which is raised differently according to the amount of users transmitting at maximum transmit power.

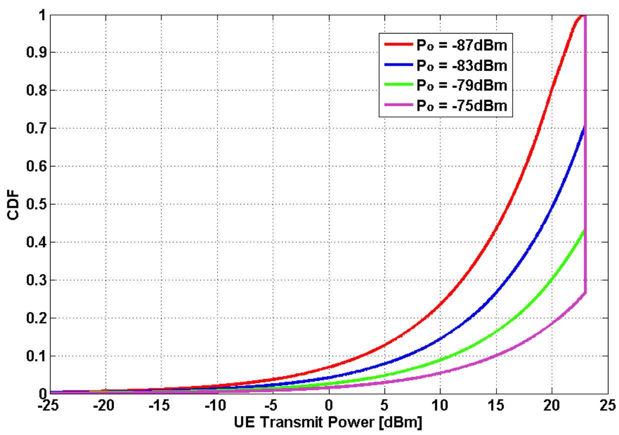

Figure 4-5 CDF of UE transmit power as a function of different $\boldsymbol{P}_0$ values

The CDF of the UE transmit power in Figure 4-5 illustrates that an increase in P_0 results in more power limited users in the system. By considering Figure 4-4, which shows average IoT levels, it can be stated that changing the P_0 value from -87 dBm to -83 dBm boosts the IoT level more compared to other P_0 increments. This phenomena is due to the fact that cell-edge users are already mostly overpowered after the P_0 setting of -83 dBm. This might give an insight that less than 30 % of users transmitting with maximum power may lead to a reasonable interference level in the system.

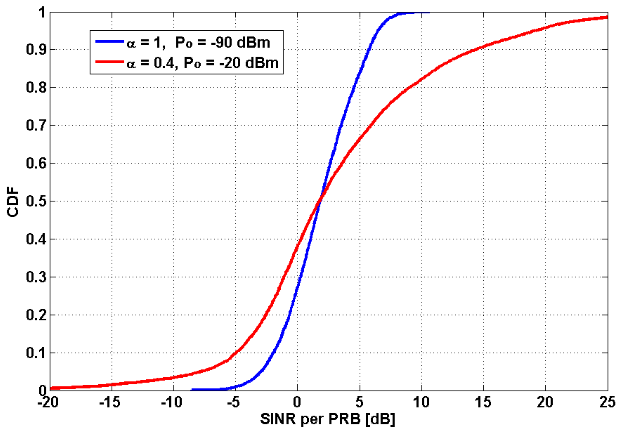

Figure 4-6 CDF of SINR per PRB with different α values

Aiming at a constant average IoT level, different P_0 values are obtained for α =1 and α =0.4 cases. From Figure 4-6, it can be seen that a lower α value spreads the SINR curve which results in a larger differentiation in terms of the SINR distribution between cell-edge and cell-center users. Therefore, it becomes important to set an appropriate P_0 value when the compensation factor α is defined less than 1 to obtain rational cell edge performances.

From this section, it is natural to conclude that there is a strong relationship between P_0 and α over the SINR and IoT distributions.

4.5.2 Performance evaluation rationale

Two Macro cell cases are defined by 3GPP for the interference and noise limited scenarios. Macro1 (case 1) is used for ISD 500 m which corresponds to an interference limited scenario and Macro3 (case 3) is used for ISD 1732 m which equates to a noise limited scenario.

The rationale behind the parameter settings for different scenarios is based on the cell capacity and cell coverage with a consideration of the corresponding acceptable average interference over thermal level in the system adopted from [25]. An acceptable IoT level is set according to the eNodeB receiver dynamic range limitations.

4.5.3 Performance in interference limited scenario

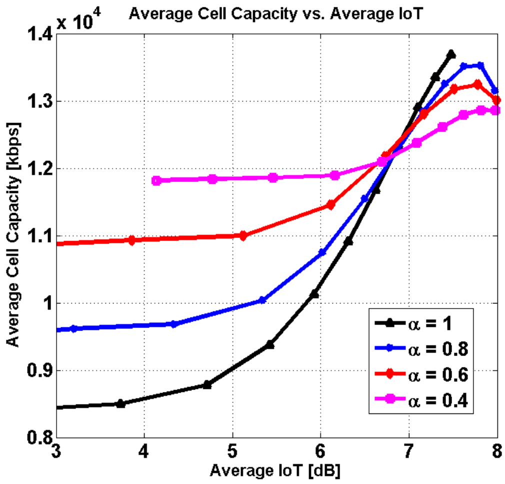

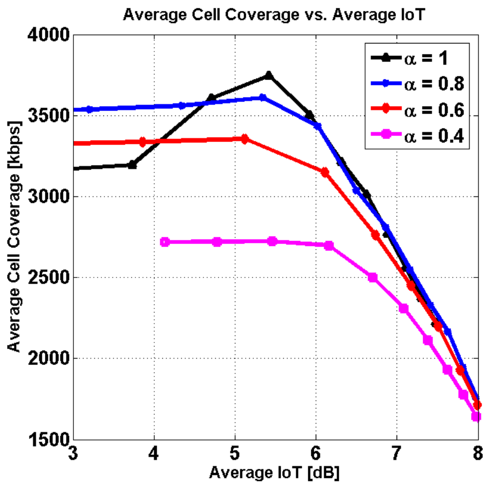

Figure 4-7 Cell capacity and coverage as a function of Average IoT

The performance of fractional power control (FPC) is shown in Figure 4-7. Plots demonstrate the average cell capacity and the average cell coverage with respect to the average IoT levels for different values of α in the Macro1 scenario. Each point along the lines corresponds to different P_0 values. The average cell capacity is calculated as the total capacity per TTI averaged over the number of iterations. The average cell coverage is calculated as the 5 %ile user throughput multiplied by the number of users per sector.

It can be observed that FPC provides higher average cell capacity up to a certain IoT level with the cost of lower cell edge performance compared to a full compensation power control (FCPC) case in which α is set as 1.

As was mentioned earlier in the parameter setting rationale section, an acceptable IoT level is a crucial concern to define the appropriate settings. Figure 4-8 illustrates that the receiver dynamic range is subject to variation according to the different average IoT levels that change with the P_0 values.

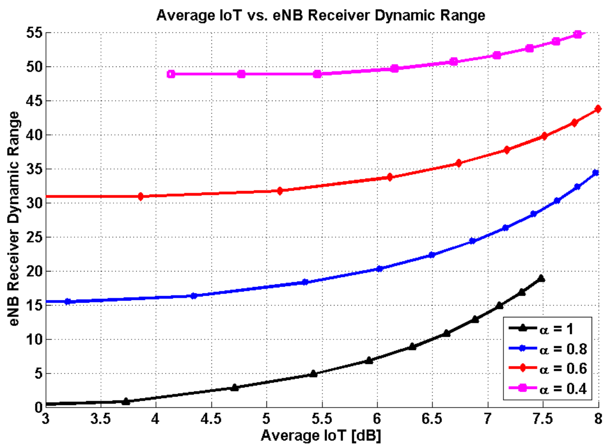

Figure 4-8 eNodeB receiver dynamic range as a function of average IoT

It is assumed that a maximum allowed receiver dynamic range at the receiver is given as 35 dBm. Thus, compensation factors lower than 0.6 do not seem to be suitable for use because of the non-acceptable receiver dynamic ranges. The IoT level that can be allowed by the $\alpha = 0.6$ setting can be a maximum of 6.5 dB in this case.

This parameter setting can be decided with respect to a compromised performance relation between the cell capacity and cell outage, while it can also be executed as a trade-off decision which depends on the priority of the cell outage or cell capacity.

A suboptimal setup for the Macro1 scenario, according to the priority selection, is suggested in Table 4-2.

	Cell outage prioritized (FCPC)	**Cell capacity prioritized (FPC)**
P_0 **[dBm] &** α	**-83 & 1**	**-40 & 0.6**
Average IoT **[dB]**	**5.4**	**6.1**
Cell capacity [kbps]	**9354**	**11442**
Cell coverage [kbps]	**3757**	**3152**

Table 4-2 Suboptimal parameter settings for Macro1 scenario

Elaboration of the settings shows that the FPC results in a 22% gain over the FCPC in cell capacity while it penalizes a gain of 16% in cell outage.

Since FPC maintains a good performance gain in cell capacity, a modified parameter setting can also be suggested to enhance cell outage as well as to slightly decrease the cell capacity for it. The selection of P_0=-42 dBm in the FPC case provides a better cell outage with only 11 % penalization compared to FCPC, while still maintaining 18% gain in cell capacity. Consequently, a low e-NodeB receiver dynamic range can also be obtained.

On the other hand, the $\alpha = 0.8$ case provides the closest results to a full compensation case, especially for outage performance. However, the $\alpha = 0.8$ will not be chosen for evaluation in order to examine the effects of FPC in a clearer way.

4.5.4 Performance in noise limited scenario

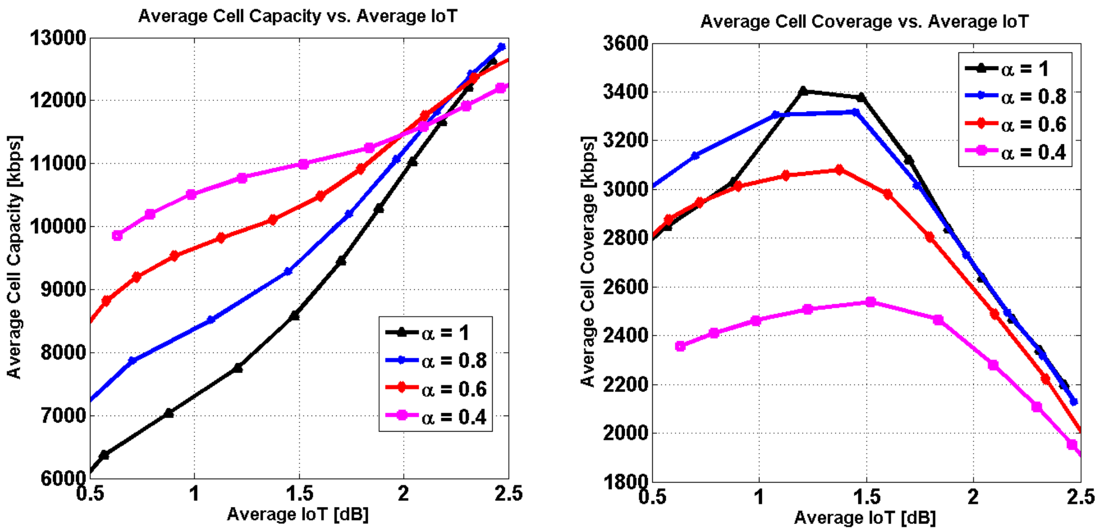

Figure 4-7 Cell capacity and coverage as a function of average IoT

The benefits of the fractional power control algorithm for the Macro3 case are not as visible as for the Macro1 case. The results, however, demonstrate similar behavior. The ***IoT*** level is now decreased due to the noise limited scenario. For a certain level of interference, for example, an ***IoT*** over 2dB, most of the cell edge users already transmit using the maximum transmit power which results in similar performance while the pathloss compensation factor is decreased (except for the 0.4 case). Again, if the cell capacity is prioritized, fractional power control provides better results, however not as gainful as for the Macro1 case.

By taking into account the eNB receiver dynamic range, a suboptimal configuration, as a trade-off between cell capacity and cell coverage, would be advisable as in Table 4-3.

	Cell outage prioritized (FCPC)	Cell capacity prioritized (FPC)
P_0 [dBm] & α	-104 & 1	-54 & 0.6
Average IoT [dB]	1.2	1.4
Cell capacity [kbps]	7815	10546
Cell coverage [kbps]	3403	3083

Table 4-3 Suboptimal parameter settings for Macro3 scenario

It should be noted that the suboptimal power control configuration obtained in eNB-only scenarios is not same with the related work [25]. This is mainly due to the shadow fading margin setup in the simulator. Throughout the simulations, the shadow fading margin is set to 0. Thus, the suboptimal P_0 values are around 13 dB higher compared to [25].

5 UPLINK POWER CONTROL IN RELAY ENHANCED LTE-A NETWORKS

In this chapter, the performance evaluation of *relay enhanced cells* is given. The performance enhancement in the uplink transmission of relay enhanced LTE-A networks by means of *power control* is investigated.

5.1 Performance evaluation of relay enhanced cells (RECs)

Relay node deployment can be used, in particular, to improve both the capacity and/or coverage for the cell edge users due to the low experienced SINR caused by propagation loss. The coverage extension procedure through relay nodes in LTE has been studied in [17]. In this present work, a fixed deployment scenario is considered in which the relay nodes are placed at the cell edges of each sector in a regular hexagonal cell layout.

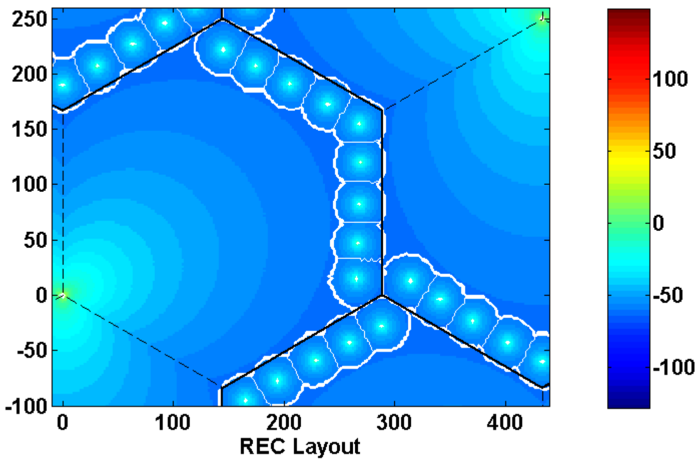

Figure 5-1 Relay node deployment representation which shows the coverage areas according to the received signal power in the downlink

The idea is to deploy the relay nodes at the cell edges in order to improve the performance of the users that experience heavy pathloss as well as minimize the cell outage. Figure 5-1 shows the coverage areas of relay nodes in REC with one-tier of RNs in each sector according to the received signal powers in downlink. In the simulations conducted during this research, the radio access point selection in the uplink transmission is assumed to be based on the downlink received power. The UEs are served by the eNBs or RNs according to the highest downlink received signal power level that is obtained from different access points.

A study that represents the SINR and the user throughput distributions is carried out to investigate the performance of relay enhanced cells.

5.1.1 Simulation assumptions

A reuse one network where each eNB and RN transmits over the whole system bandwidth and interferes with each other is considered.

The latest channel models of 3GPP for direct link and access link are used which are defined in [18]. The relay link between the RNs and eNBs is assumed to be ideal. The Macro1 (ISD 500m) scenario is applied and different maximum transmit power levels for the eNBs, RNs and UEs are selected according to the latest 3GPP evaluation proposal. Directional antennas for the eNBs and omni-directional antennas for the RNs are used. In each sector, 48 users are uniformly distributed and 200 iterations are performed to collect satisfying statistics.

A detailed simulation assumptions table that consists of all parameters can be found in Appendix C.

5.1.2 Simulation results

Relay based deployment has been studied in this part with one, three and five RNs deployed at the cell edge of a hexagonal cellular layout.

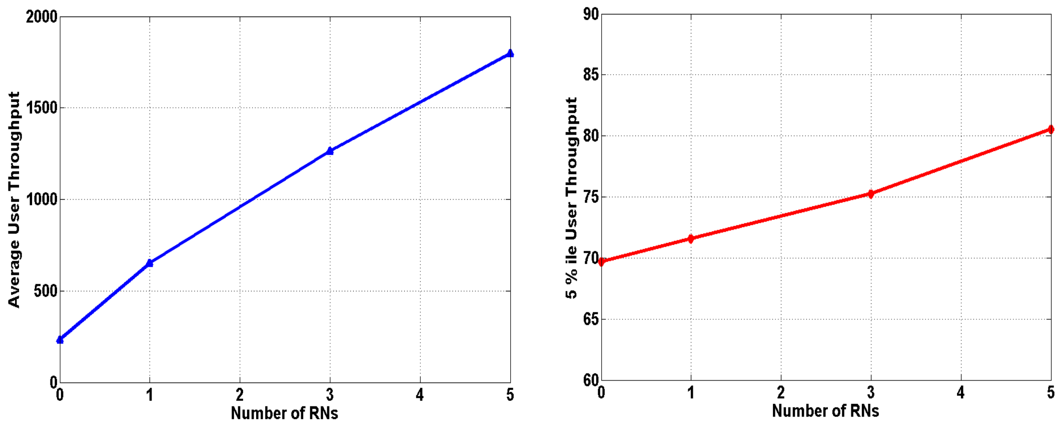

Figure 5-2 Average user throughput and 5% ile user throughput as a function of number of RNs deployed in the sector

The simulation results show that relay based deployment improves the throughput of each user in the cell as can be seen from Figure 5-2. The average user throughput is boosted by the relay nodes. This is mainly due to the nature of OFDMA based resource allocation applied at the RNs. Each RN serves a few UEs within its coverage area which then results in greater PRB allocation for each of the UEs. Finally, this is transformed into high user throughputs. More than a 100 % gain is observed in the sector when the number of relay nodes increase. However, it should be taken into account that the relay link is assumed to be working ideally in this work.

The relay based system also manages to improve the outage performance despite the fact that it introduces extra cell edges which generates additional interference from maximum powered users connected to the RNs.

Power control becomes vital particularly when a reuse one system is applied as in this work. The latest approved pathloss channel models of 3GPP for REC are used. It is observed that the channel model used in access link has a heavier pathloss compared to the direct link channel model. Thus, interferences in the uplink transmission that are generated from the access link to the direct link are higher than those generated from the direct link to the access link proportionally. Therefore, with an excellent power control scheme that is applied for the users connected to the RNs, performance of the UEs served by the eNBs can be further enhanced. The next section will discuss this topic in more detail.

5.2 Performance evaluation of three-tier REC with full compensation power control (FCPC) and fractional power control (FPC)

The new cell edges introduced by the RNs consisting of high power UEs will lead to severe intra-cell and inter-cell interference -in particular, when a high number of relay nodes are deployed in the cell with reuse one. For this reason, power control becomes an important means in the uplink transmission of REC for mitigating the interference and increasing the cell edge and system performance. The standardized LTE uplink power control scheme should be investigated in relay based deployment to achieve an optimal performance.

5.2.1 Evaluation methodology and parameter settings

In this part, an investigation of fractional power control and full compensation power control in relay based deployment is performed. The eNB-only deployment with optimal parameter settings for coverage and capacity limited scenarios have been assumed as a reference case for performance evaluation in the REC scenario. Notations are as follows:

- **FCPC** : optimal parameter setting for full compensation power control in eNB-only deployment (coverage prioritized case)
- **FPC** : optimal parameter setting for fractional power control in eNB-only deployment (capacity prioritized case)
- **FCPC (eNB and RN)** : optimal parameter setting for full compensation power Control (FCPC) in eNB-only deployment is applied in relay based deployment both at the eNB and RN
- **FPC (eNB and RN)** : optimal parameter setting for fractional power control (FPC) in eNB-only deployment is applied in relay based deployment both at the eNB and RN

Scenario	α at eNB	P_0 at eNB	α at RN	P_0 at RN
eNB-only with FCPC	1	-83 dBm	-	-
eNB-only with FPC	0.6	-42 dBm	-	-
FCPC (eNB and RN)	1	-83 dBm	1	-83 dBm
FPC (eNB and RN)	0.6	-42 dBm	0.6	-42 dBm

Table 5-1 Parameter settings for FCPC and FPC

Parameter settings that are used at the initial simulations for relay based deployment are given in Table 5-1.

5.2.1.1 UE transmit power distribution

Transmit power distribution should be analyzed after relay node deployment in the system prior to seeing the results. The power control parameters P_0 and α obtained for eNB-only deployment are used for the relay based deployment. It should be taken into account that most of the users transmitting with maximum power are at the moment connected to RNs. However, other users that still remain connected to eNBs are now getting more PRBs.

Thus, the power control formula is affected by this change and the percentages of users transmitting at maximum transmit power is expected to alter.

Power control scheme		**UEs using max power connected to eNB**	**UEs using max power connected to RNs**
FPC (eNB and RN)	eNB-only	9 %	-
	one-tier REC	10 %	47 %
	two-tier REC	11 %	42 %
	three-tier REC	13 %	37 %
FCPC (eNB and RN)	eNB-only	30 %	-
	one-tier REC	17 %	10 %
	two-tier REC	15 %	5 %
	three-tier REC	14 %	3 %

Table 5-2 Power distribution of UEs after RN deployment

It is observed that the number of UEs transmitting at maximum power changes after RN deployment is adopted. The maintained parameter settings from the eNB-only deployment results in a low number of UEs at power limitation for FCPC whereas a high number of UEs at power limitation for FPC at RNs. The analysis shows that small changes in the percentages of UEs transmitting at maximum power do not have a noticeable impact on the results. Furthermore, the FPC case, where around 40 % of the UEs at the RNs were transmitting with maximum power, is expected to have noticeable performance degradation for the UEs at the eNBs due to high interference.

5.2.2 Results for FPC in three-tier REC

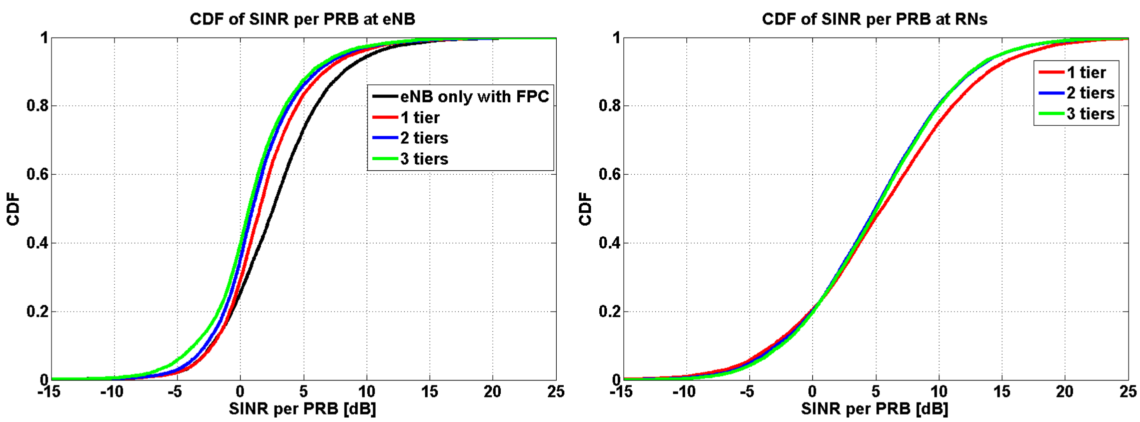

Figure 5-3 CDF of SINR per PRB at eNB and RNs for the different number of deployed RN tiers in FPC (eNB and RN) case

Figure 5-3 shows the SINR distributions at the eNB and RNs. It demonstrates that relay based deployment decreases the experienced SINR per PRB at the eNB due to the fact that interference caused by the users connected to RNs is getting significant. It should be also noted that power control parameters for the users connected to RNs are not adjusted after relay based deployment. This clearly shows that an optimal power control setting performed for RNs can maintain a close performance to the eNB-only scenario for the users connected to the eNBs, or even improve the performance. It should be kept in mind that the simulated scenario is a worst case scenario in which 48 users are uniformly distributed over the cell area where 22 % of the users are served by 9 RNs forming the first tier deployed in the cell edge. Therefore, each RN serves at least one user in its coverage area that results in higher interference compared to a light cell load case.

The CDF of SINR per PRB at RNs plot illustrates that interference among the RNs is not relevant in general. A similar SINR distribution is maintained for a different number of deployed RN tiers.

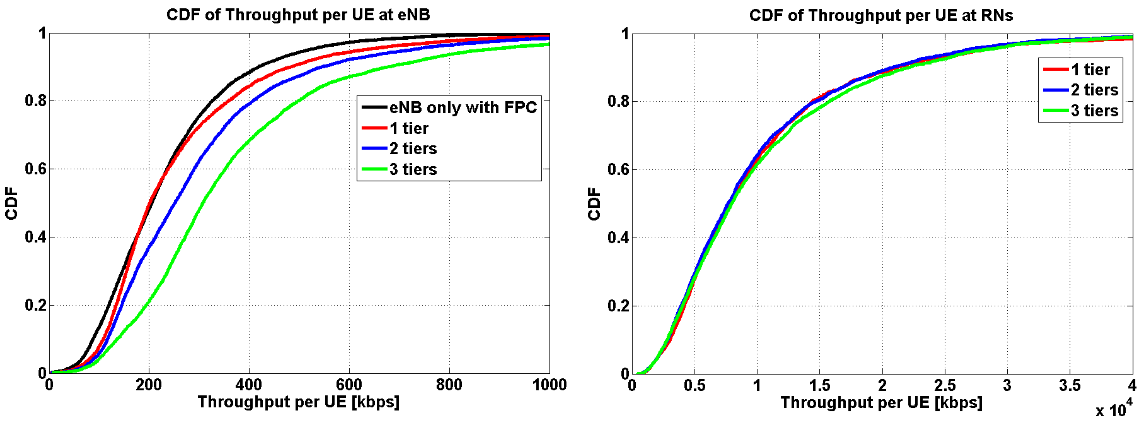

Figure 5-4 CDF of Throughput per UE at eNB and RNs for the different number of deployed RN tiers in FPC (eNB and RN) case

In Figure 5-4, the CDF of throughput per UE at the eNB plot shows that RN deployment increases the throughput performance of the users connected eNBs, apart from an exception around 50 % ile of the CDF curve in the one-tier RN deployment case which is due to the suffering users that experience high interference from the users connected to the RNs. This improvement can be explained by the fact that the worse users which are connected to the eNBs in the earlier case are now served by the RNs a the cell edges; therefore, the assigned numbers of PRBs for the users connected to the eNBs increase by 22 %, 40 % and 56 % respectively according to the number of tiers used. This can be translated into higher throughput with more bandwidth allocation for the UEs served by the eNBs.

On the other hand, the CDF of throughput per UE at the RNs plot resembles the SINR per PRB plot where the number of deployed tiers does not significantly alter the results. Therefore, similar throughput distribution among the users connected to RNs with different tiers can be observed from Figure 5-4. However, very high throughput is experienced by the users connected to the RNs compared to the users connected to the eNB due to the fact that the RNs are mostly serving one or two users in their coverage areas which results in a very large resource allocation for each user that is finally transformed into high capacity.

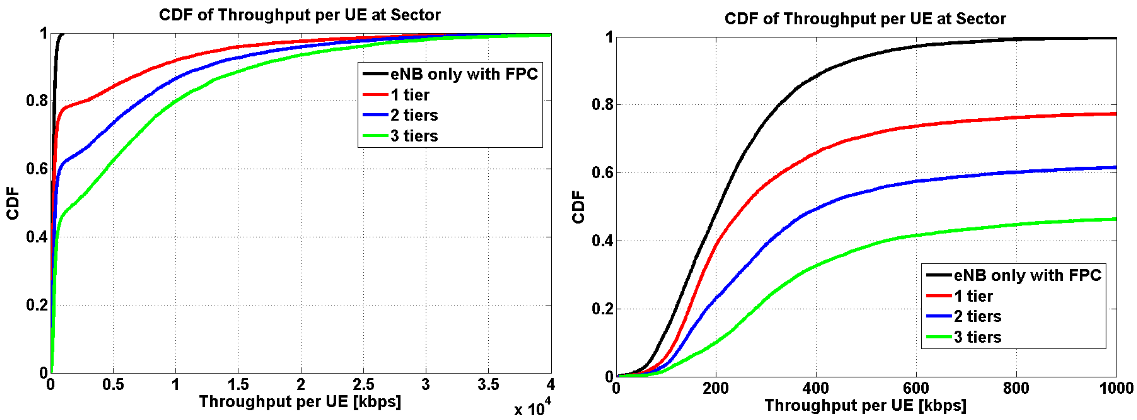

Figure 5-5 CDF of Throughput per UE at sector for the different number of deployed RN tiers in FPC (eNB and RN) case

Finally, the CDF of throughput per UE at the sector that combines the whole user statistics is given in Figure 5-5. The CDF curve is obtained by a combination of user throughput values that are experienced separately both at the eNB and RNs. It should be noted that the figure given on the right side illustrates the low throughput profile of the same figure given on the left. As can be observed from these figures, relay node deployment outperforms eNB-only deployment both for cell edge throughput and cell capacity. Adding more relay nodes basically improves not only the edge user throughput but also the total cell capacity compared to an eNB-only scenario.

Since this work is not related to cost analysis of eNBs or RNs relations according to site densities which achieve required performance for relay enhanced cells, it can be concluded that it is advisable to deploy as many relay nodes as possible in the considered deployment scenario to improve the cell performance. For a detailed cost analysis study of relay enhanced cells the reader is referred to [29].

5.2.3 Comparison of FPC and FCPC in three-tier REC

The previous section revealed the performance of fractional power control in a three-tier relay enhanced cell with a revised parameter setting from an eNB-only scenario. It has been observed that similar behavior for the experienced SINR and user throughputs are also obtained with FCPC. Thus, it is interesting to compare the related results of FCPC and FPC in terms of user throughput including a reference scenario of eNB-only deployment with FPC.

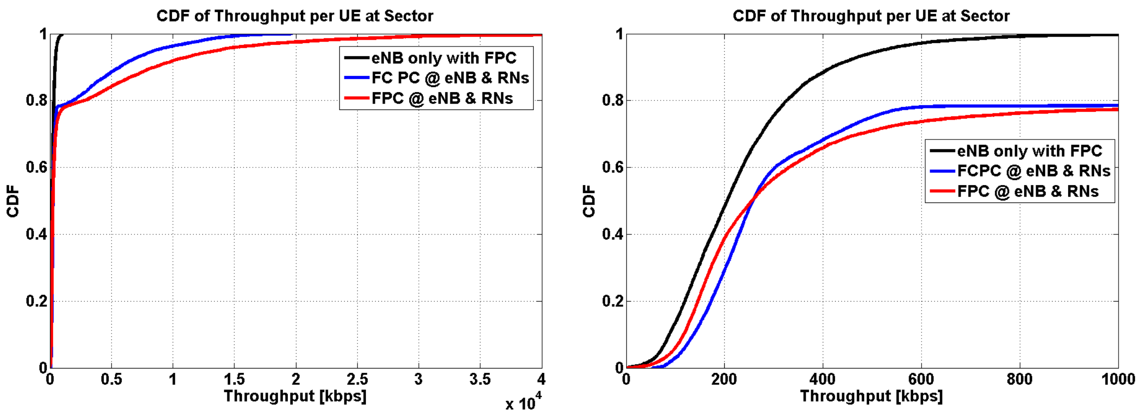

Figure 5-6 CDF of throughput per UE at sector for FCPC (eNB and RN) vs. FPC (eNB and RN) in one-tier REC

The user throughput at sector curves given in Figure 5-6 can be regarded in a way that a lower percentile of the curve is formed of users connected to the eNB and a higher percentile of the curve is made up users connected to RNs. The figure that is shown on the right side is the scaled version of the one which is given on the left. It is scaled so that the low percentile user throughputs can be examined.

The parameter settings which are extended from the eNB-only scenario in one-tier REC scenario shows that FCPC provides higher throughput for the users connected to the eNB up to 50 %ile of the CDF curve, whereas FPC boosts the performance of the users connected to the RNs. Furthermore, the FCPC also provides better user throughputs at the eNB reaching to 80 %ile.

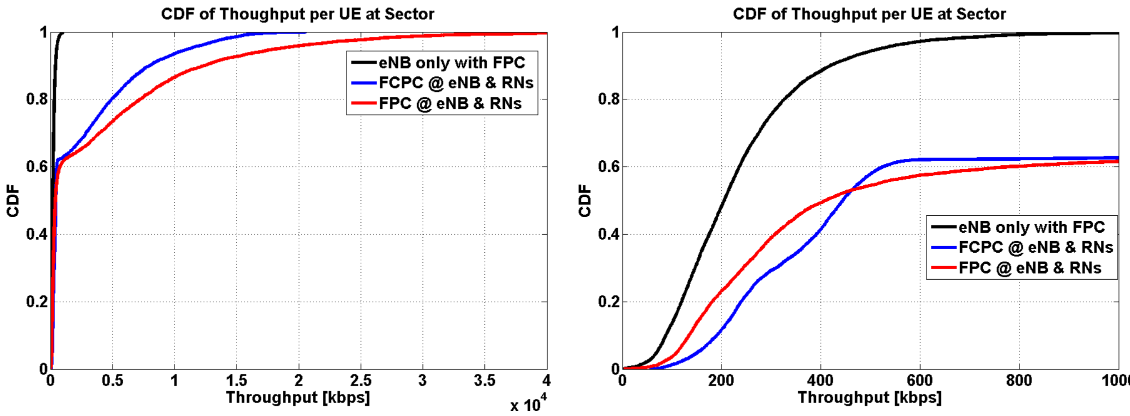

Figure 5-7 CDF of throughput per UE at sector for FCPC (eNB and RN) vs. FPC (eNB and RN) in two-tier REC

The results shown in Figure 5-7 with two-tier of RN deployment resemble the previous case. A general throughput improvement for all of the users can be observed. A trade-off point that indicates the breakeven point of the two curves can be mentioned to differentiate the performance of FPC and FCPC. The trade-off point between FCPC and FPC is still around a 50 %ile of the CDF curve here –just as in the one-tier case.

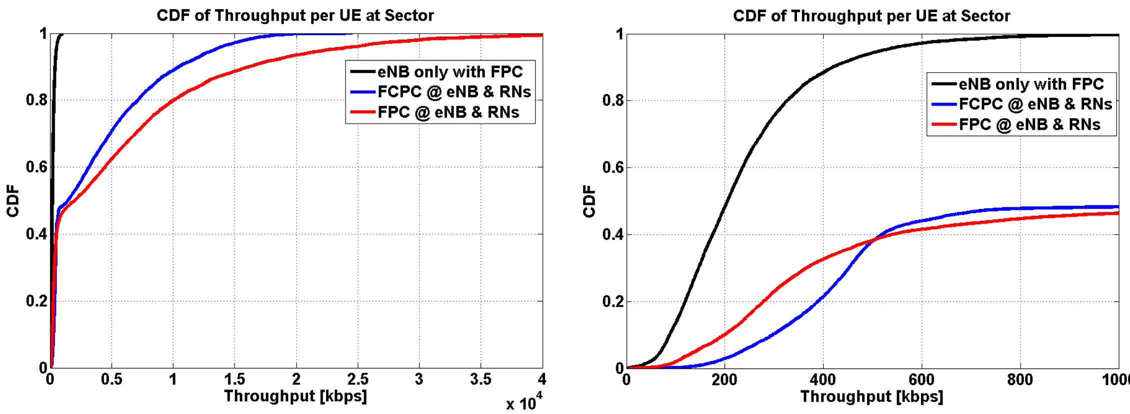

Figure 5-8 CDF of throughput per UE at sector for FCPC (eNB and RN) vs. FPC (eNB and RN) in three-tier REC

In Figure 5-8, the three-tier REC scenario resulted in the highest capacity as was seen in Section 5.2.2. The performance difference between FCPC and FPC becomes more visible with more tiers. An average capacity gain of 8 % for the users connected to the eNB with FCPC in two-tier deployment now increases to an average capacity gain of 10 % with three tiers deployment. A similar gain effect with FPC is also valid for the users connected to RNs.

Consequently, the overview of the simulated results can be listed as follows:

- Three-tier RN deployment outperforms one-tier and two-tier RN deployment with better 5 %ile user throughput performance and higher capacity in the sector.
- An investigation of user load in the cell has shown that RN deployment can also lead to better SINR distributions for all the users in a light cell load. For a detailed evaluation, consult Appendix D.
- FCPC results in a higher throughput for most of the users connected to eNBs whereas FPC outperforms FCPC for the users connected to RNs.
- Parameter settings should be re-adjusted after RN deployment.
- FCPC would be initially considered as a good way to try to obtain parameter settings in relay enhanced cells.

5.3 Performance improvement with optimal settings in one-tier REC

In this section, parameter optimization is studied in one-tier REC in which full compensation power control is applied both at the eNB and RNs. As a reference for performance evaluation, an eNB-only deployment scenario with FPC is considered.

5.3.1 Analysis of P_0 at eNB

Analysis consists of statistics in which the P_0 value is fixed at RNs and it is altered at eNBs. The P_0 value for the users connected to RNs is set to -83 dBm.

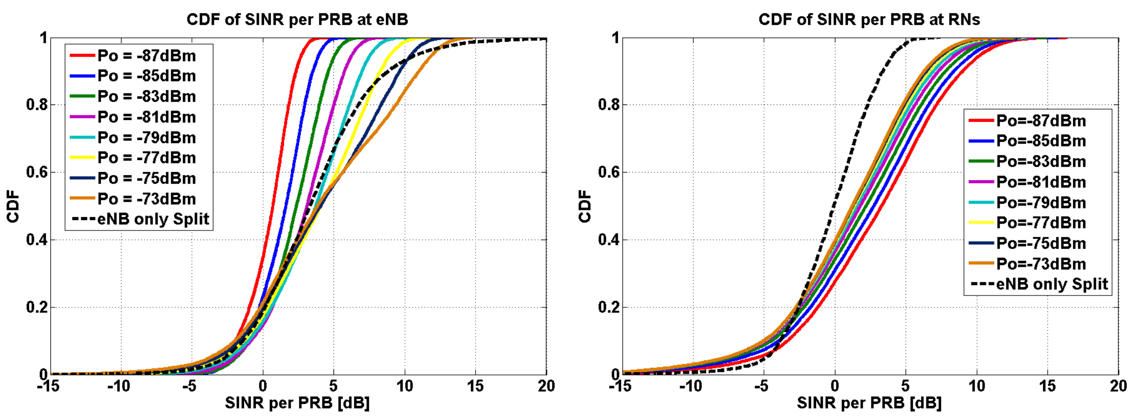

Figure 5-9 CDF of SINR per PRB at eNB and RNs as a function of changing P_0 at eNB

Firstly, it should be noted that the reference scenario curves in Figure 5-9 are now different to the previous ones. The SINR curves are separated to show only cell edge and cell center users in order to see the effects of relay node deployment more clearly. In the left side figure, the eNB-only split curve only includes the statistics of the cell center users without considering the area that is covered by RNs. Yet again, in the right side figure, the eNB-only split curve includes only the statistics of the cell edge users.

The CDF of the SINR per PRB at the eNB illustrates that an optimal P_0 setting (-83 dBm) for the eNB-only scenario still provides the highest 5 % ile SINR. However, an increase of P_0 results in a slight 5 % ile performance decrease but also as a considerable gain in the SINR of all the other PRBs at the eNB. Moreover, the SINR distribution at RNs is not effected significantly because of higher transmit power of the users connected to eNBs due to the bad access link channel. It is also seen that an unnecessary high SINR per PRB at RNs can be slightly decreased.

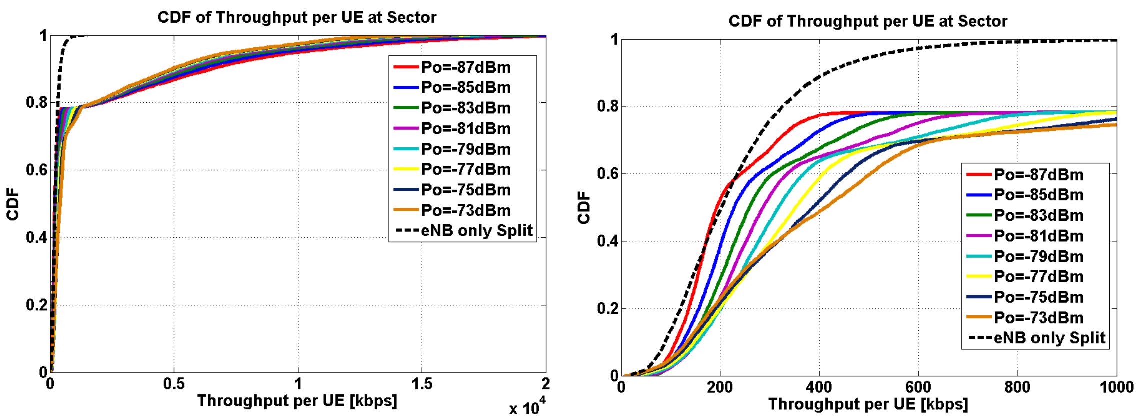

Figure 5-10 CDF of throughput per UE at sector as a function of changing P_0 at eNB

In Figure 5-10, the throughput per UE plots are given. It should be noted that the two figures are the same but different scales are used to show the performance of cell edge users more clearly on the right side which demonstrates similar results to the SINR plots. The high throughput experienced by the users connected to the RNs can be decreased by increasing the P_0 value for the users served by the eNB. This results in a throughput gain for the region between 20 % and 80 % of the CDF curve by slightly penalizing the 5 %ile user throughput at the eNBs.

The conclusion is that optimization of P_0 at the eNB does not drastically impact the performance of the users connected to the RNs since these users already experience a comparatively high throughput. On the other hand, optimum cell edge performance can still be maintained with the suboptimal settings found in the eNB-only scenario.

5.3.2 Analysis of P_0 at RN

The analysis consists of statistics in which the P_0 value is fixed at eNBs and it is altered at RNs. The P_0 value is set to -83 dBm at eNBs.

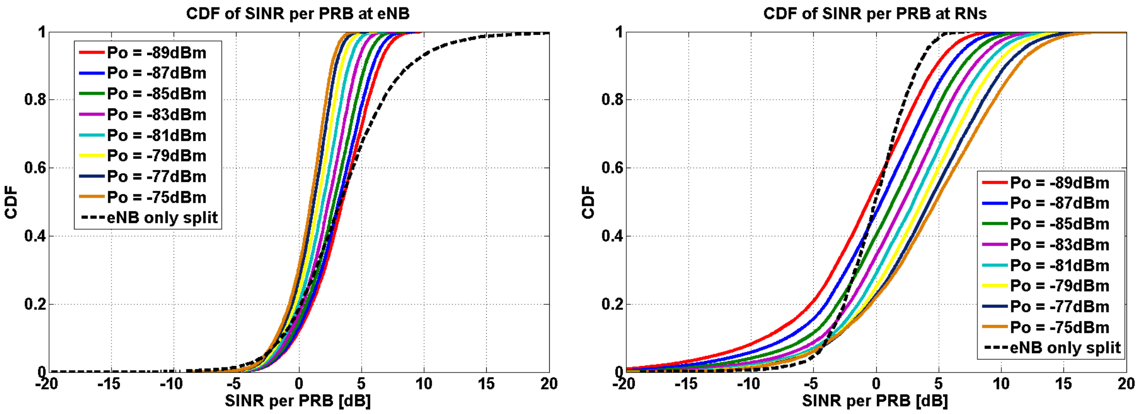

Figure 5-11 CDF of SINR per PRB at eNB and RNs as a function of changing P_0 at RNs

As it was expected, it is possible to further enhance the SINR of the users connected to the eNB by selecting the P_0 appropriately for the users connected to the RNs. Figure 5-11 shows that a lower P_0 value at RNs, which then leads to an overall power decrease for all the users served by the RNs, results in SINR decrement at the RNs. It, however, improves the SINR of the users served by the eNB. It has been noticed in the previous investigations that users at the eNB mostly experience low throughputs. Thus, it is necessary to increase their performance.

The P_0 value can be decreased as much as possible at RNs that still satisfy the users experience low SINR connected to RNs in order to improve the performance of the users served by eNBs. The blocking probability of the users connected to RNs becomes a crucial issue in this case. In this current work, however, the size of blocking probability that can be supported in the network is not considered. An SINR threshold of around -15 dB is assumed for the RNs to obtain a reasonable blocking probability. Finally, since the throughout mapping results in high capacity for the users served by RNs due to large resource allocation, the SINR threshold which is defined by P_0 can be set as small as possible.

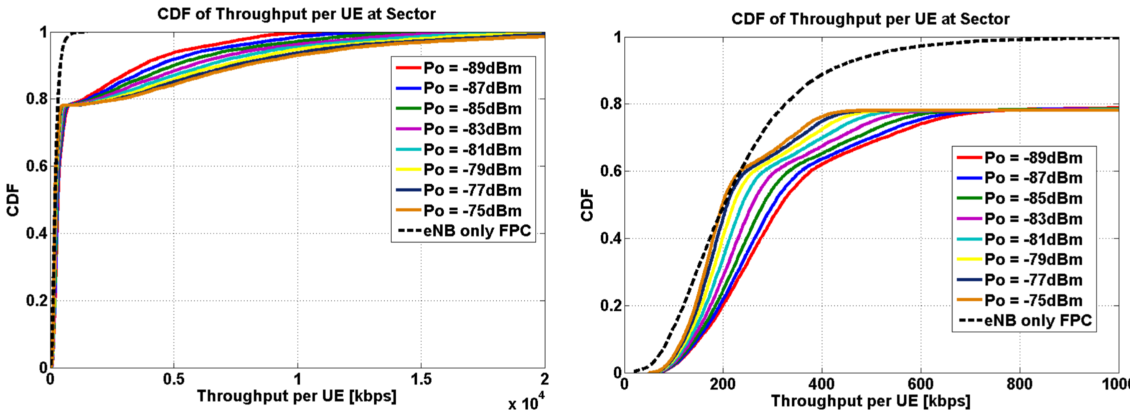

Figure 5-12 CDF of throughput per UE at sector as a function of changing P_0 at RNs

Figure 5-12 shows the CDF of throughput per UE at the sector. It demonstrates that high throughput is reduced at RNs by selecting a lower P_0 value. This also provides higher throughput for the users connected to eNBs. Compared to the previous case where the P_0 value is altered at eNBs, the throughput increase at the eNB does not now result in a 5 %ile user throughput penalization. An overall throughput increase can be obtained for all of the users served by eNBs by means of an overall power decrease for all of the users connected to RNs.

Therefore, it becomes important to find the optimal choice of P_0 value when the relay node deployment enters the scenario considering the average and 5 %ile user throughputs.

5.3.3 Maximum allowed transmit power with no PC at RNs

Usage without any power control at RNs is considered for investigation in this section. The idea was to investigate whether it would be possible to maintain the SINR performance of the users connected to RNs with a fixed maximum allowed transmit power that will also lead to both a higher throughput for the cell center users as well as a simpler RN design without penalizing the users served by eNBs.

Three different maximum allowed transmit power settings are considered for the users connected to RNs and they are compared with the reference scenario FCPC (eNB and RN). The considered power limitations are listed as follows:

- Maximum Tx power = 18 dBm
- Maximum Tx power = 15 dBm
- Maximum Tx power = 13 dBm

It should be taken into account that transmit power of each user is already decreased even if a power control scheme is not applied for this investigation. According to the fixed 18 dBm, 15 dBm and 13 dBm maximum transmit power settings; transmit power of each user decreases by 3.2, 6.3 and 10 times respectively compared to typical maximum transmit power level (23 dBm). It should be also noted that the use of no power control will lead to higher receiver dynamic ranges at RNs. It is observed that receiver dynamic ranges of RNs are around 35-40 dBm without power control usage.

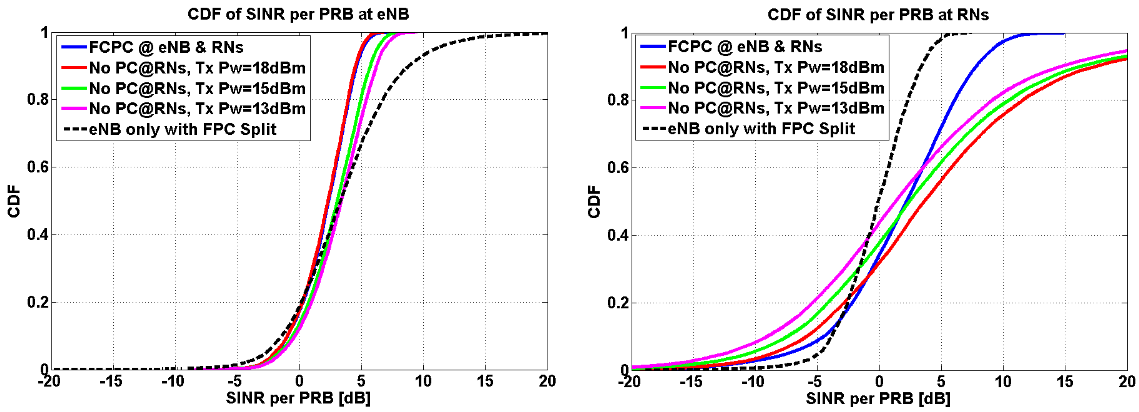

Figure 5-13 CDF of SINR per PRB at eNB and RNs as a function of different maximum allowed Tx power levels without PC at RNs

In Figure 5-13, the CDF of SINR per PRB at the eNB plot shows that similar performance of FCPC case can be obtained with a maximum transmit power setting of 18 dBm at RNs and it can be improved by lower maximum transmit power settings such as 15 dBm and 13 dBm respectively.

The CDF of the SINR per PRB plot at RNs illustrates that a 5 %ile performance similar to the FCPC case can be maintained with a fixed 18 dBm maximum transmit power setting. On the other hand, the SINR curves are more spread without power control. Users that experience a low SINR are penalized and the users that experience a high SINR are improved by the use of no power control. Since the idea is to improve the performance of the low SINR experienced users at eNBs by increasing their throughputs, the maximum transmit power for the UEs at RNs can be set as small as possible which still satisfies the users that experience a low SINR with a reasonable blocking probability.

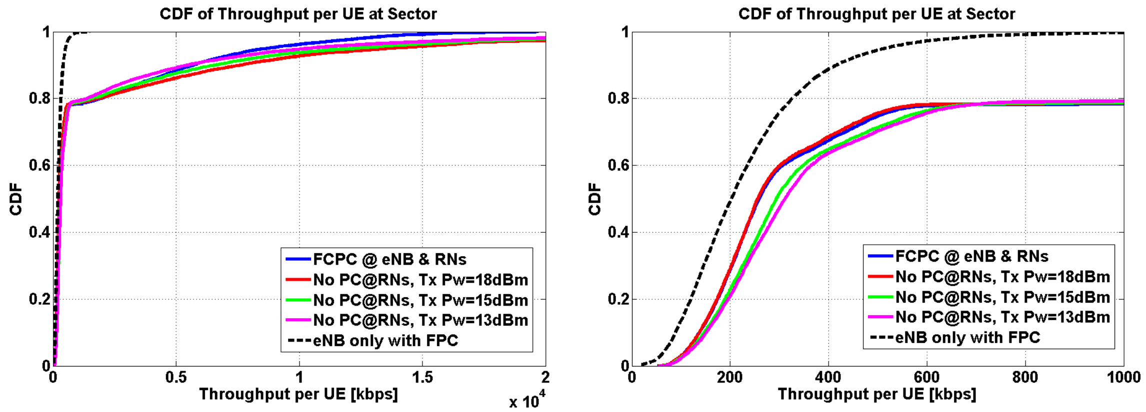

Figure 5-14 CDF of throughput per UE at sector as a function of different maximum allowed Tx power levels without PC at RNs

As can be seen from the CDF of throughput per UE plots in Figure 5-14, a maximum transmit power setting of 18 dBm which provides same performance for the users served by eNBs results in higher capacity for the users connected to RNs. Thus, the maximum transmit power configuration of the users that are served by RNs provides similar improvement to the previous investigation in which the P_0 value is decreased at RNs.

In conclusion, the use of no power control at RNs can be considered as a good candidate for simple implementation and operation procedure as long as an appropriate initial maximum transmit power setting is executed for the UEs connected to RNs by taking into account the receiver dynamic ranges of the RNs.

On the other hand, the P_0 settings with a maximum transmit power limitation can be still re-adjusted to reduce the experienced high user throughput at RNs and enhance the user throughput at eNBs. The next section will discuss this approach in detail.

5.3.4 Maximum allowed transmit power with PC at RNs

Investigation of the re-adjustment of the P_0 setting with an allowed maximum transmit power for the users connected to RNs is carried out in this part. A suboptimal maximum transmit power setting of 15 dBm is considered as a reference and three different P_0 settings are used for the performance evaluation.

It should be noted that a decrease in P_0 value after a fixed allowed maximum transmit power setup mainly decreases the power of cell center users served by RNs.

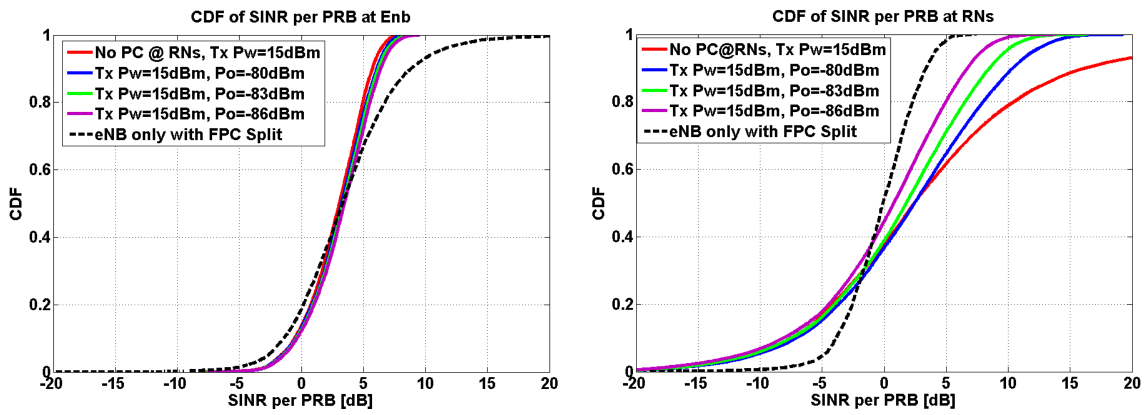

Figure 5-15 CDF of SINR per PRB at eNB and RNs as a function of different maximum allowed Tx power levels with PC at RNs

As can be seen from the CDF of SINR per PRB at the RNs plot in Figure 5-15, lower $\boldsymbol{P}_0$ values maintain the cell edge performance and decrease the performance of cell center users served by RNs which then leads to a SINR improvement for the users served by the eNB which is seen on the left side.

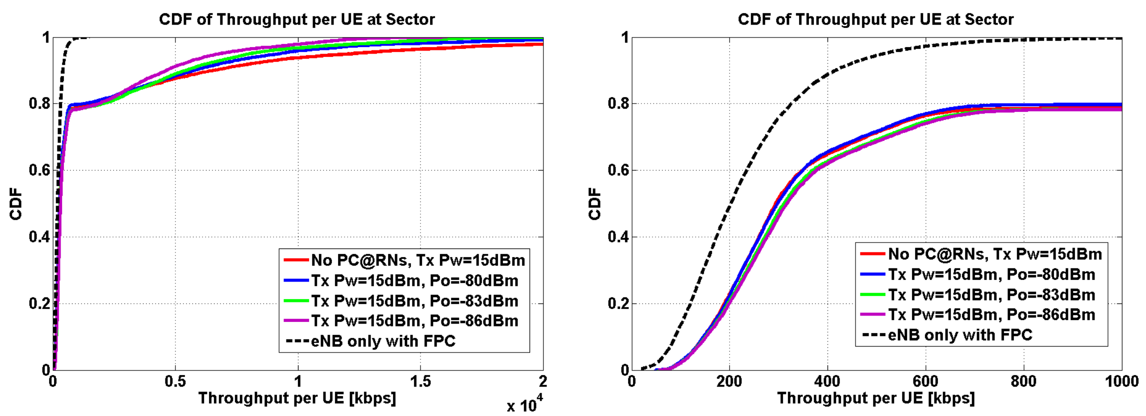

Figure 5-16 CDF of throughput per UE at sector as a function of different maximum allowed Tx power levels with PC at RNs

The results obtained for throughput per UE are as expected. A high throughput of users connected to RNs is now decreased by a proper $\boldsymbol{P}_0$ setting. Therefore, users that are connected to the eNB experience higher throughput compared to the reference scenario.

If it is required to evaluate the results in terms of performance improvement according to the plots, it can be observed that an average capacity enhancement of 6 % is achieved at the eNB compared to the reference scenario in which no PC with maximum transmit power of 15 dBm is considered at RNs. Moreover, an average of capacity enhancement of 20 % is also obtained at the eNB compared to the FCPC (eNB and RN) case.

It is expected that the effects of P_0 configuration with a fixed maximum allowed transmit power case will not be visible in FPC as much as is shown for FCPC. This is due to the fact that fractional power control already decreases the SINR of cell center users by decreasing the P_0. Therefore, setting a lower maximum allowed transmit power and then decreasing the P_0 will very slightly impact the SINR distribution for the cell center users in the FPC case.

5.3.5 Comparison of FPC and FCPC with optimized settings

Performance evaluation based on parameter settings at eNBs and RNs with full compensation power control has been demonstrated in previous sections. It is appropriate to extend the evaluation case for fractional power control as well. Therefore, the results of suboptimal re-adjusted parameter settings for FPC in one-tier relay based deployment are compared with the formerly improved FCPC case in this section.

Firstly, it is observed that the FPC (eNB and RNs) case which was previously evaluated does not provide a performance close to optimal. It was shown in Section 5.2.1.1 that the extended P_0 settings that are also used for the users connected to RNs results in a very high SINR and throughput at the RNs and, correspondingly, a very low SINR and throughput at the eNB. Therefore, a decrease in the P_0 value at RNs is expected to lead to a promising performance enhancement for the FPC case compared to the FCPC case.

Suboptimal settings	**Setting 1**		**Setting 2 (with max Tx power)**	
Parameters	*eNB*	*RNs*	*eNB*	*RNs*
α	0.6	0.6	0.6	0.6
P_0 **(dBm)**	-42	-52	-42	-54
Max Tx power (dBm)	23	23	23	15

Table 5-3 Optimized suboptimal parameter settings for FPC in one-tier REC

The suboptimal parameters setting obtained for FPC in a one-tier REC which leads to similar lower SINR values at RNs relative to the optimal configuration of FCPC with a maximum transmit power with PC is found and demonstrated in Table 5-3.

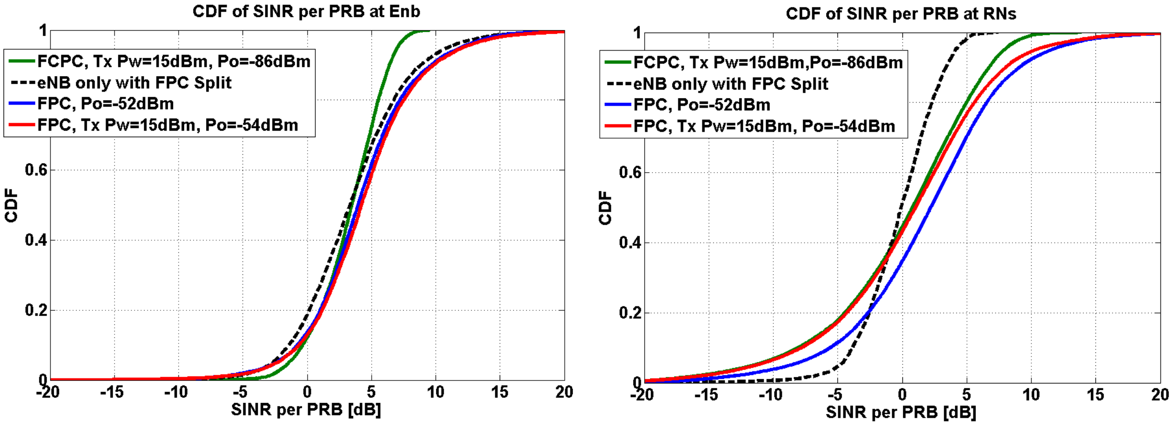

Figure 5-17 CDF of SINR per PRB at eNB and RNs with re-optimized suboptimal configurations of FPC (eNB and RN) and FCPC (eNB and RN)

In Figure 5-17, the CDF plot of the SINR per PRB at the eNB shows that new parameter settings adjusted for FPC provides a higher SINR of around 90 % of the PRBs except the cell edge users under a 10 % percentile. Yet, it is also seen that the maximum transmit power limitation setting for the users at RNs slightly improves the performance of users served by the eNB, whereas it decreases the experienced SINR at the RNs.

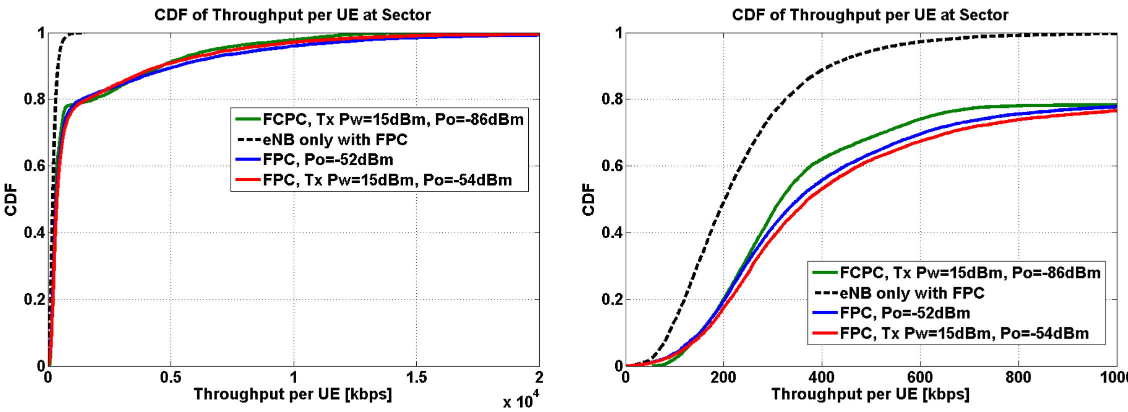

Figure 5-18 CDF of throughput per UE at sector with re-optimized suboptimal configurations of FPC (eNB and RN) and FCPC (eNB and RN)

In Figure 5-18, the user throughput results illustrate that suboptimal settings of the FPC outperforms the FCPC in general. To understand the results in a better way, Table 5-4 and Table 5-5 that contain the performance evaluation respectively for 5 %ile user throughput and mean user throughput including also the first reference cases FPC and FCPC are given.

5 % ile user throughput (kbps)	**eNB-only with FPC**	**FCPC (eNB and RNs)**	**FPC (eNB and RNs)**	**FCPC TxPW=15dBm P_0 = -86dBm**	**FPC TxPW=15dBm P_0 = -54dBm**
eNB	70	107	87	116	109
RNs	-	1591	2099	1534	1386
Sector	70	113	95	122	120

Table 5-4 5 %ile user throughput

As can be observed from Table 5-4 and Table 5-5, the re-adjusted power control parameter settings after relay based deployment provides better performance compared to extended parameter settings from the eNB-only deployment.

Mean user throughput (kbps)	**eNB-only with FPC**	**FCPC (eNB and RNs)**	**FPC (eNB and RNs)**	**FCPC TxPW=15dBm Po = -86dBm**	**FPC TxPW=15dBm Po = -54dBm**
eNB	235	250	261	302	369
RNs	-	6285	10312	5112	5792
Sector	235	1544	2463	1355	1556

Table 5-5 Mean user throughput

The performance evaluation of optimized suboptimal settings is as follows:

The FPC with appropriate settings results in a negligible 5 %ile performance penalizing which is only 2 % lower performance compared to FCPC with appropriate settings. However, the FPC improves the mean user throughput for all of the users in the cell area. The users at the eNB experience a 23 % higher mean throughput and the users at the RNs experience a 13 % higher mean throughput compared to the FCPC case. The mean user throughput values are enhanced by 15 % in the sector by means of the appropriate suboptimal FPC configuration both at the eNBs and RNs.

So far we have studied the performance evaluation and the performance improvement via parameter optimization of the LTE uplink power control scheme for REC in the Macro1 scenario in which the interference is the limiting factor for the performance.

Throughout this work, a Macro3 noise limited scenario with 1732 m ISD is also investigated and given in Appendix E.

6 CONCLUSIONS AND FUTURE WORK

This chapter summarizes the main conclusions of this work and presents possible areas for improvements. Further works that can be performed are also described briefly.

6.1 Conclusions

Uplink power control in Relay Enhanced Cells (RECs) within the LTE framework was discussed in this thesis. Power control is one of the most important RRM functionalities for improving system capacity, mitigating interference and reducing power consumption. The uplink transmission scheme of LTE named as SC-FDMA does not produce the intra-cell interference and near far effect similar to WCDMA. However, the system is still sensitive to inter-cell interference. In LTE, Fractional Power Control (FPC) is used to improve the uplink performance as it utilizes a compensation factor for the pathloss and it is introduced to improve the performance of cell center users by inducing an acceptable level of inter-cell interference.

Before studying the power control at the RECs, performance evaluation of fractional power control for the LTE uplink transmission was carried out in Chapter 4. Two suboptimal parameter settings were obtained based on the priority of capacity and coverage in Macro cell scenario. The results suggest that better capacity can be obtained through lower compensation factors in FPC while traditional Full Compensation Power Control (FCPC) provides better cell edge performance.

Heterogeneous cell deployment was applied with fixed RN deployment where one, two or three tiers of relays were used at the cell edges of each sector in a hexagonal cellular network. The uplink fractional power control formula was used in each RN. The eNB-only deployment with optimal parameter settings related to the capacity prioritized scenario by FPC was taken as a reference case for the performance evaluation in the REC. The initial parameter settings in the REC were defined as FPC (eNB and RNs) and FCPC (eNB and RNs) where the optimal settings of FPC and FCPC in the eNB-only scenario were applied both at eNBs and RNs. It was found that user throughput in the REC is improved as the number of RNs increases regardless of the relay link overhead. The user throughput results demonstrate that FPC and FCPC have a trade-off point which varies slightly depending on the number of relay tiers used. The trade-off point indicates the breakeven point of two curves to differentiate the performance of FPC and FCPC. It is observed that FCPC provides better performance for the user throughput less than 50 % ile of the CDF curve, whereas FPC boosts the performance for the remaining users in the sector. On the other hand, FCPC also provides higher user throughput than FPC up to 80 % ile of the CDF curve at eNBs.

Analysis of $\boldsymbol{P}_0$ was performed both at eNBs and RNs in a one-tier REC. The $\boldsymbol{P}_0$ setting at eNB in the REC shows that a suboptimal $\boldsymbol{P}_0$ setting defined in the eNB-only scenario can be still maintained to provide optimum cell edge performance for the users served by eNBs in a REC. On the other hand, the $\boldsymbol{P}_0$ settings at RNs show that a defined $\boldsymbol{P}_0$ setting in the eNB-only scenario does not offer optimum performance. A decrease of the $\boldsymbol{P}_0$ value at RNs results in a general power down for all the users leading to SINR and throughput increase for the users served by the eNBs. It was discussed that by aiming for threshold value of a -15 dB SINR at RNs, the $\boldsymbol{P}_0$ value can be set as small as possible. In particular, a 12 dB lower $\boldsymbol{P}_0$ value provides up to 35 % gain in the average user throughput at eNBs as well as decreasing the excessive high user throughput at RNs for the FPC case.

Power control might still be regarded as an extra overhead at RNs. Therefore, another analysis which suggest for no power control by considering a fixed maximum allowed transmit power at RNs was examined. The results illustrate that a fixed maximum value of 18 dBm transmit power provides similar cell edge performance to the FPC (eNB and RNs) and FCPC (eNB and RNs) cases with a throughput enhancement for the cell center users.

Moreover, configuration of the $\boldsymbol{P}_0$ with maximum allowed transmit power can be re-adjusted further. Thus, parameter settings were optimized for FPC and FCPC, leading to similar cell edge performance with target of around a -15 dB SINR threshold at RNs in a one-tier REC. Furthermore, the results illustrate that users served by the eNBs are improved by 8.5 % and 25 % for the 5 %ile user throughput in FCPC and FPC, respectively. The average user throughput at the eNB is also increased by 17 % for FCPC and 41 % for FPC according to the re-optimized configurations.

It was also observed that FPC outperforms FCPC with an appropriate parameter optimization and transmit power setup. The average user throughput at eNB, the average user throughput at RNs and the average sector user throughputs are improved by 23 %, 13 % and 15 % respectively with use of the FPC instead of the FCPC.

In conclusion, this research verifies that the standardized fractional power control formula for LTE is feasible to use in REC scenarios. Parameter optimization and transmit power setup are important for achieving optimal performance. Optimized configuration brings a 15 % capacity improvement by means of FPC compared to FCPC for similar cell edge performance.

6.2 Future work

This thesis presented a general study of uplink power control in relaying enhanced LTE. An insight into understanding power control in REC was gained from this study. However, relay link overhead should be taken into account for evaluating more realistic scenarios and enhanced channel models will be needed.

Reuse one was applied between the direct link and access link. Threshold values for SINR were used to tune the parameters and it was noticed that excessive user throughputs were experienced at RNs. A resource partitioning scheme, however, which provides interference isolation between users of eNBs and RNs with less resource allocation for the access link could provide better SINRs for RNs. Moreover, the relay link implementation results have shown that resource allocation -and possibly some frequency reuse- would be necessary with an accurate power control configuration to enhance the system.

The use of different scheduler could improve the system performance. A scheduler that allocates less PRBs for the cell edge users both at eNBs and RNs, with acceptable throughput threshold maintenance, could mitigate the intra-cell and inter-cell interferences and also increase the total capacity in the cell.

Furthermore, in [31] Overload Indication (OI) and High Interference Indication (HII) per PRB was introduced to report both interference overload and interference sensitivity. An investigation of dynamic power control parameter configuration based on HII and/or OI to organize the interference coordination by means of closed loop parameters can be performed. This would provide interesting input to LTE development after which ideas could be generated for REC scenarios.

7 APPENDICES

7.1 Appendix A - Transmission parameters for SC-FDMA LTE uplink

Table 7.1 that shows the transmission parameters for SC-FDMA LTE uplink FDD mode is given.

Transmission BW		1.4MHz	3.0MHz	5.0MHz	10MHz	15MHz	20MHz
Slot duration (frame structure type 1)		0.5ms	0.5ms	0.5ms	0.5ms	0.5ms	0.5ms
Subcarrier spacing		15kHz	15kHz	15kHz	15kHz	15kHz	15kHz
Sampling frequency		30.72MHz	30.72MHz	30.72MHz	30.72MHz	30.72MHz	30.72MHz
Length of SC-FDMA symbol in time units* (excluding CP)		2048	2048	2048	2048	2048	2048
Number of occupied resource blocks		6	15	25	50	75	100
Number of occupied subcarriers		72	180	300	600	900	1200
Number of SC-FDMA symbols per slot	Normal CP	7	7	7	7	7	7
	Extended CP	6	6	6	6	6	6
Cyclic prefix (CP) length (frame type 1) where I is the symbol position in a slot	Normal CP	160 for I=0 144 for I=1 to 6	160 for I=0 144 for I=1 to 6	160 for I=0 144 for I=1 to 6	160 for I=0 144 for I=1 to 6	160 for I=0 144 for I=1 to 6	160 for I=0 144 for I=1 to 6
	Extended CP	512 for I=0 to 5	512 for I=0 to 5	512 for I=0 to 5	512 for I=0 to 5	512 for I=0 to 5	512 for I=0 to 5

Table 7-1 Transmission parameters for SC-FDMA LTE uplink

7.2 Appendix B - System model and default simulation parameters

Appendix B overviews the features of the system model used in this thesis work. The default simulation parameters and assumptions applied through the simulations are also summarized.

7.2.1 Cellular network model

According to the 3GPP evaluation methodology report [18], the cell layout used in this work consists of Macro1 as well as Macro3 reference cases. Grid size is formed of 19 sites with 3 hexagonal sectors in each. A single site refers to the area covered by one eNB. Sectorization is applied by directional antennas at each eNB. The inter-site distance (ISD) is the distance between two sites which is defined as 500 m for the Macro1 case and 1732 m for the Macro3 case.

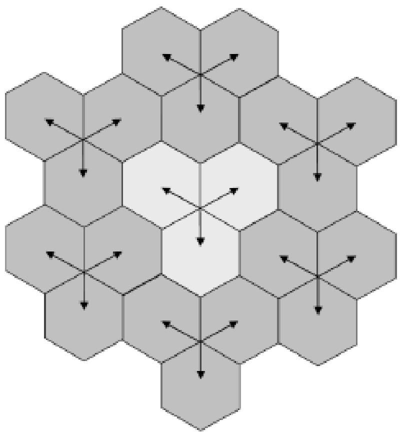

Figure 7-1 eNB-only cell layout

Relay enhanced cells (REC) are simulated in this work. Relay nodes are deployed at the cell edges of each sector to provide good coverage for the users close to the cell border.

RNs are considered to be deployed below rooftop level (5 meters) such as on lampposts with omni-directional antennas, whereas eNBs are deployed above rooftop level (25 meters) with directional antennas.

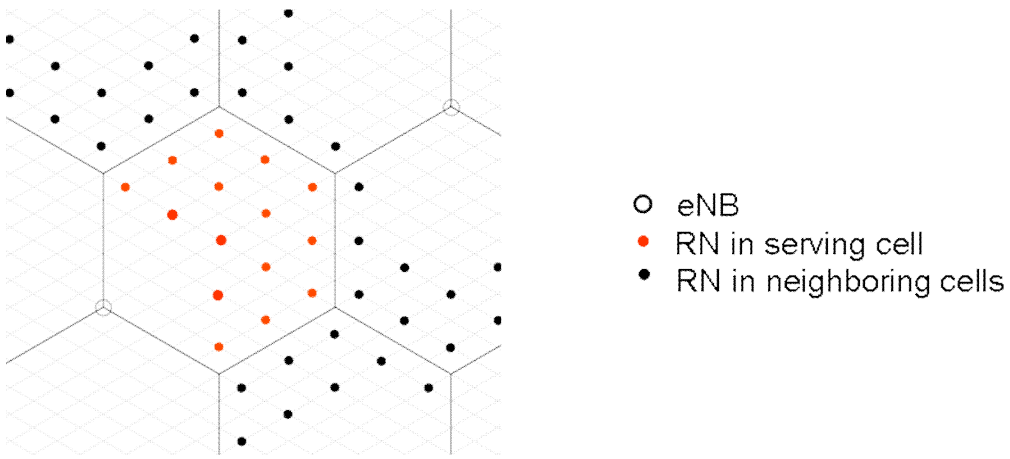

Figure 7-2 REC layout

Figure 7-2 illustrates the relay based deployment scenario in which RNs are deployed starting from cell edges towards the cell center geometrically.

The ISD between the RNs is calculated in a geometric way so that coverage areas of RNs collide as little as possible and the cell edges of eNBs are covered as efficiently as possible without any non-served areas remaining.

7.2.2 Propagation model

The latest channel models for heterogeneous cell deployment are adopted from [18]. The propagation model consists of distance attenuation and antenna gain. Shadowing and fast fading are not considered. For simplicity in link budget calculations, margins can be used to take into account the shadowing and cable losses.

Distance dependent pathloss models for the direct link, the relay link and the access link are given as follows:

- Direct Link (eNB to UE)

$$\boldsymbol{L} = 128.1 + 37.6\,\mathbf{log}_{10}\,\boldsymbol{R} \qquad (\boldsymbol{f} = 2\boldsymbol{GHz},\ \boldsymbol{R}\ \text{in km})$$

- Relay Link (eNB to RN)

$$\boldsymbol{L} = 124.5 + 37.6\,\mathbf{log}_{10}\,\boldsymbol{R} \qquad (\boldsymbol{f} = 2\boldsymbol{GHz},\ \boldsymbol{R}\ \text{in km})$$

- Access Link (RN to UE)

$$\boldsymbol{L} = 140.7 + 36.7\,\mathbf{log}_{10}\,\boldsymbol{R} \qquad (\boldsymbol{f} = 2\boldsymbol{GHz},\boldsymbol{R}\ \text{in km})$$

The relay link is considered as ideal in this work. Uplink user transmission occurs among UEs to eNBs or UEs to RNs. The relay link in between the RNs and eNBs is assumed to be perfectly modeled. Therefore, capacity results obtained at RNs are transferred to eNBs without any loss. On the other hand, the relay link overhead is also studied in a separate section.

Antenna configurations	**Tx**	**Rx**
UE	1	2
eNB	2	2
RN	2	2

Table 7-2 Antenna configurations

Antenna configurations are assumed as given in Table 7-2 according to [18].

The spatial processing is applied at eNB antennas. The antenna pattern defined in the 3GPP evaluation report is used as the following:

$$A(\theta) = -\min\left[12\left(\frac{\theta}{\theta_{3dB}}\right)^2, A_m\right] \quad (A_m = 25,\ \theta_{3dB} = 70 \text{ degrees})\ [\text{dB}]$$

Omni-directional antennas at RNs and cross polarized antennas at UEs are considered without antenna pattern gains.

7.2.3 System model

The system model includes factors such as transmission bandwidth, carrier frequency, maximum transmission powers, frequency reuse, as well as packet scheduler and modulation methods, among other parameters.

Uplink operation bandwidth is assumed as 10 MHz formed of 50 PRBs each with a bandwidth of 180 KHz. Then, 48 PRBs are used for data transmission and 2 PRBs are separated for control channels. The uplink data frame is composed of 10 transmission time intervals (TTI) and each TTI is defined as 1 ms.

The carrier frequency is assumed as 2 GHz.

The defined 3GPP radio access point (RAP) power classes [18] are used as maximum transmission powers for eNBs, RNs and UEs which are given as 46 dBm, 30 dBm and 23 dBm respectively.

The frequency reuse factor is assumed as 1 in which each eNB and RN transmits over the complete system bandwidth and interferes with each other. Resource partitioning is not applied. Thermal noise is modeled as PSD for each PRB given as N = 174 dBm / Hz.

A round robin (RR) packet scheduler is used in which users uniformly share the transmission bandwidth as a first-come, first-served manner. Depending on the simulated number of users (8 or 48 will be explained in the next section) each user is assigned to either 6 PRBs or 1 PRB.

The link adaptation is performed based on adaptive modulation and coding according to the LTE hulve curve approximation. Since the simulations are static and performed mostly only for one TTI, a simple link adaptation can be assumed to be applied.

7.2.4 User and traffic model

User generation is applied in a randomly placed manner in each sector according to a uniform distribution. User distribution is equally balanced in the sectors so that each sector has the same number of users. Only the statistics of the users in the first sector of the center site is collected to evaluate the results.

User drops per sector is applied as 8 users or 48 users in which 1000 and 200 iterations are performed respectively to collect sufficient statistics from the first sector.

The serving BS or RN of a given UE in the uplink is decided according to the downlink received signal power.

The traffic model is assumed to be full buffer uplink. The duplexing scheme is used as FDD since only one TTI is simulated. Throughout the investigations of relay link overhead, an FDD-TDD mode is applied and two TTIs are simulated.

7.2.5 Throughput mapping

The modulation and coding scheme (MCS) is selected according to the experienced SINR for the users in the LTE uplink. Higher SINR results in higher order modulation and coding rates.

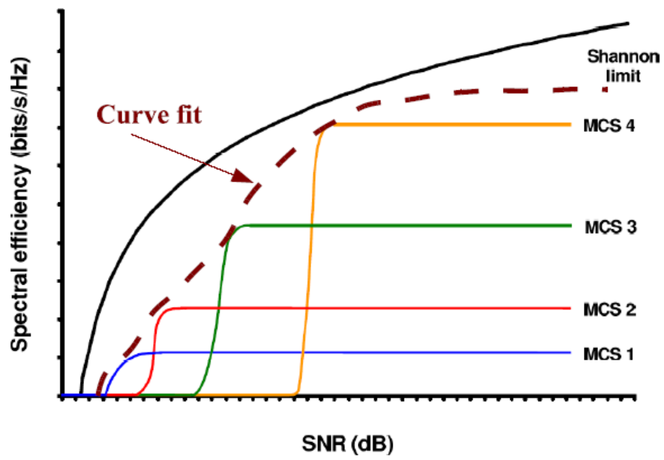

Figure 7-3 LTE Hull curve approximation

Figure 7-3 shows how the different MCS are chosen considering the experienced SINR.

Throughput calculation for a given user is performed in accordance with its experienced SINR and its allocated bandwidth by means of an enhanced Shannon formula by the LTE hull curve approximation with efficiency terms:

$$C = BW_{eff} \cdot M \cdot BW_{PRB} \times \log_2(1 + (\frac{SINR}{SINR_{eff}})) \quad \text{[bps]}$$

where:

BW_{eff} : is the bandwidth efficiency. It is used as 0.88.

M : is the number of allocated PRBs.

BW_{PRB} : is the bandwidth of one PRB. It is equal to 180 KHz.

$SINR$: is the user experienced SINR.

$SINR_{eff}$: is the SINR efficiency in the system. It is set to 1.25

7.3 Appendix C - Simulation parameters of REC

Baseline system simulation parameters are set according to the 3GPP text proposal for LTE-A evaluation methodology [24] and [18]. System, network and antenna parameter settings are given in Table 7-3.

System parameters

Parameter	**Default**	**Comments**
Carrier frequency	2 GHz	
Channel bandwidth	10 MHz	
Number of cells	19 (cellular hexagonal layout)	
Channel models	eNB-UE -> 3GPP TR 25.942 $L = 128.1 + 37.6 \log_{10} R$ eNB-RN -> 3GPP R1-084026 $L = 124.5 + 37.6 \log_{10} R$ RN-UE -> 3GPP R1-084026 $L = 140.7 + 36.7 \log_{10} R$	In this study the overhead due to relay link (eNB-RN) is neglected.

eNB number of antenna per sector	2	2 rx and 2 tx
RN number of antenna	2	2 rx and 2 tx
UE number of antenna	2	2 rx and 1 tx
eNB max tx power	46 dBm	
RN max tx power	30 dBm	
UE max tx power	23 dBm	
UE mobility	No	
Traffic model	Full buffer Uplink	
Simulation window	1 TTI	
Extra margin	0 dB	
Simulated instances	200	

Network layout parameters

Parameter	Default	Comments
Number of cells	19 (cellular hexagonal layout)	No wrap around and simulation results obtained considering only one sector of the cell in the center
Number of sectors per cell	3	
Number of RNs per sector	9 (1 tier) / 18 (2 tiers) / 29 (3 tiers)	
Number of UEs per sector	48	
eNB location/height	25m	Above rooftop
RN location/height	5m	Below rooftop
UE location/height	1.5m	
eNB – eNB distance	Case 1: 500m, Case 3: 1732m	
eNB – RN distance	Regular grid	

Multi antenna parameters

Parameter	Default	Comments
eNB number of antenna per sector	2	2 rx, 2 tx
eNB antenna configuration per sector	linear	

eNB antenna element spacing	0.5λ	
eNB azimuth antenna element pattern	$A(\theta) = -\min\left[12\left(\frac{\theta}{\theta_{3dB}}\right)^2, A_m\right]$ $A_m = 25$ dB, $\theta_{3dB} = 70^o$	
eNB elevation antenna gain	14 dBi	
eNB receiver noise figure	5 dB	
RN number of antenna	2	2 rx, 2 tx
RN antenna configuration	omni	
RN azimuth antenna element pattern	$A(\theta) = 0$	
RN-UE elevation antenna gain	5 dBi	
RN-eNB elevation antenna gain	7 dBi	
RN receiver noise figure	7 dB	
UE number of antenna	2	2 rx, 1 tx
UE antenna configuration	dual cross polarized antennas	
UE azimuth antenna element pattern	$A(\theta) = 0$	
UE elevation antenna gain	0 dBi	
UE receiver noise figure	9 dB	

Table 7-3 Simulation parameters

7.4 Appendix D - Some simulation results with light cell load

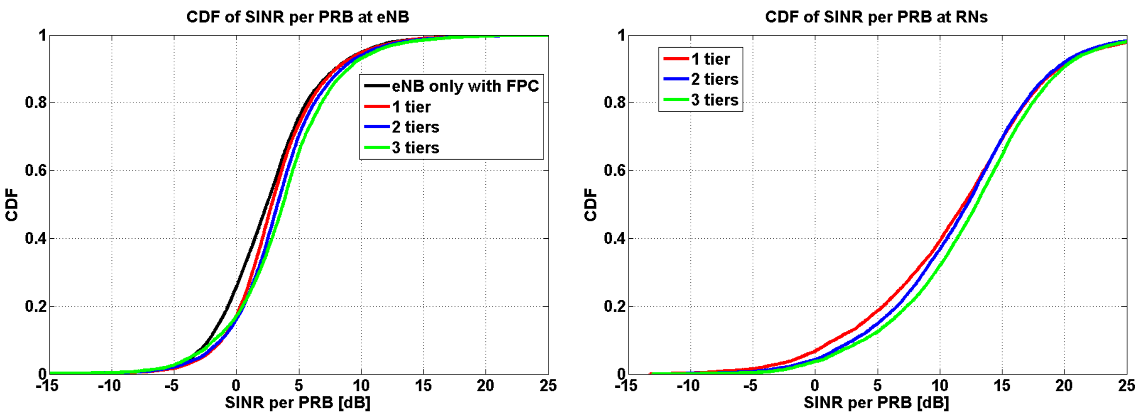

Figure 7-4 CDF of SINR per PRB at eNB and RNs for the different number of deployed RN tiers in FPC (eNB and RN) case

Under light cell load conditions, the results have shown that SINR at eNB increases by means of relay node deployment. In parallel, SINR at RN is also improved compared to a heavy loaded cell due to the effect of interference degradation.

The results suggest that the light cell load conditions allow the possibility of making more power decrease for the users served by RNs since the experienced SINR values at RNs are higher compared to the heavy cell loads. As a result, this improves the low SINR experienced by the users connected to the eNBs.

7.5 Appendix E - Performance evaluation of REC in Macro3 scenario

The results illustrate the same behavior to the Macro1 scenario. Since the system is noise limited, the effects of FPC, which is mainly used to mitigate the inter-cell interference, is not as much obvious as it is seen in the Macro1 scenario. It is expected that similar results can be obtained in the REC after parameter optimization in a Macro3 scenario.

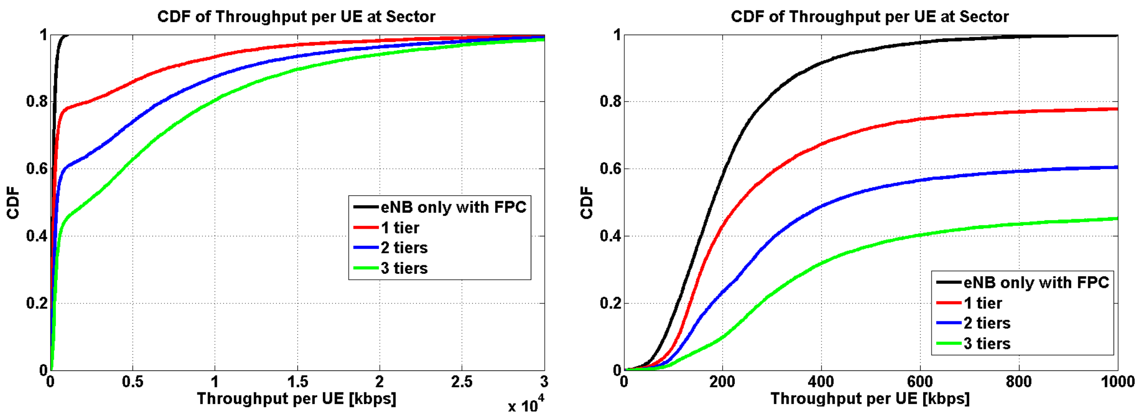

Figure 7-5 CDF of throughput per UE at sector for different number of deployed RN tiers in FPC (eNB and RN) case

As can be seen in Figure 7-5, user throughput is increased compared to the eNB-only scenario. The more RN is added to the system, the more system capacity improvement can be obtained regardless of the relay link overhead as it was in the interference limited scenario. The results resemble to the Macro1 case, however it should be noted that the user throughputs are lower.

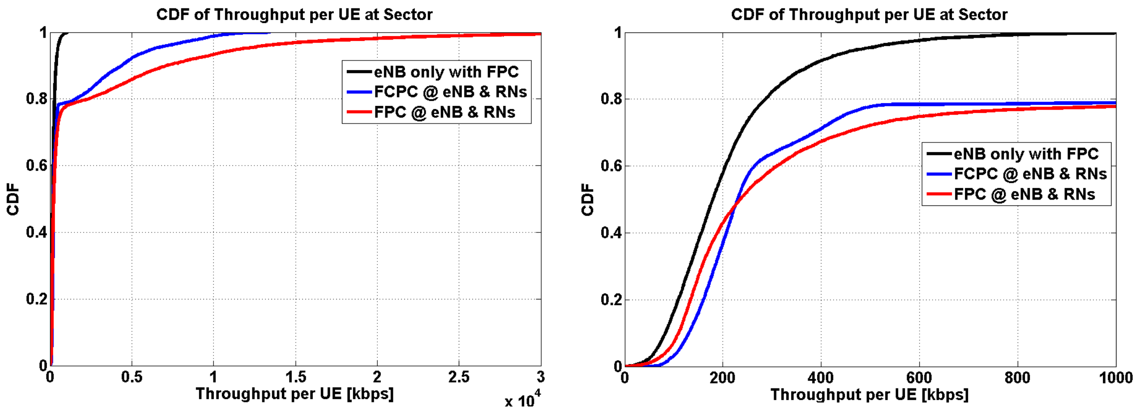

Figure 7-6 CDF of throughput per UE at sector for FCPC (eNB and RN) vs. FPC (eNB and RN) in one-tier REC

Comparison of the FCPC and FPC is given in Figure 7-6 in Macro3 scenario. Optimal parameter settings that are obtained for the eNB-only scenario are applied both at the eNBs and RNs in the REC. Similar behavior to the Macro1 is seen in the Macro3 scenario but with lower throughput in general.

It is concluded that parameter configuration can be performed in a way similar to the Macro1 case. It is anticipated that the FPC will provide more advantageous system capacity and user throughput than FCPC for the same cell edge performance after parameter optimization is properly performed.

7.6 Appendix F - Investigation of relay link

This section is included to illustrate the effects of relay link deployment on the performance in the considered scenario. Relay link has been assumed ideal in the performed simulations throughout this work. Usage of full reuse transmission in this work is applicable for an ideal relay link where UE capacity obtained at RNs is expected to be carried to eNBs without any loss. This kind of link can be maintained via microwave transmission between the RNs and eNBs. However, an optimal resource partitioning scheme can also be applied to overcome the inefficiency generated by relay link transmission.

7.6.1 Resource allocation

The following assumptions are considered in order to give the reader an idea how the relay link should be implemented. Half duplex transmission is applied to define the signal reception between the direct link and relay link. Thus, the eNB receives signals only from

UEs or RNs at one time interval. Uplink transmissions between the UE to the eNB and the UE to the RN are applied in the first TTI as it was applied in the rest of the work and reuse one is assumed so that each transmission interferes with each other. The relay link transmits in the second TTI, and the total number of PRBs is shared between each RN deployed in the sector.

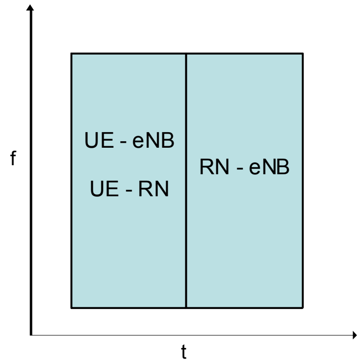

Figure 7-7 Resource allocation scheme

7.6.2 End-to-end user throughput

The following method is applied to calculate the end-to-end user throughput in the scenario considered. The user throughput in the access link transmission is available since UEs have transmitted to RNs in an earlier TTI. The number of available PRBs are shared by the number of RNs deployed in the sector in each even TTI and reuse one is applied between the RNs of each sector. The SINR per PRB is calculated for each even TTI and the capacity that can be carried by each RN is obtained according to the number of PRBs which are assigned to each RN. Then, the relay link throughput is proportionally shared by the number of users which are buffered from the access link. Finally, end-to-end user throughput is decided according to a minimum formula:

$$e2e_{UE\ Throughput} = \mathbf{min}(\text{Access Link Throughput per UE}, \frac{\text{Relay Link Throughput per RN}}{\text{Number of UEs served by RN}})$$

The cell edge user throughput increases even with the relay link as can be seen in Figure 7-8. It outperforms the eNB-only deployment. However, it is observed that the excessive user throughput which is experienced from the access link is limited by the relay link.

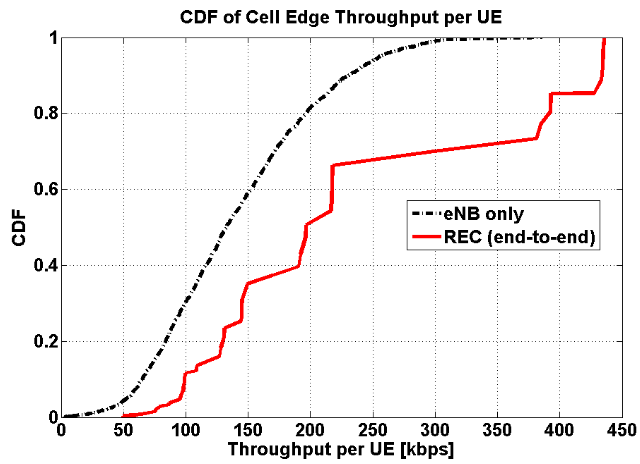

Figure 7-8 CDF of cell edge UE throughput at eNB-only and REC scenarios

The investigations carried out on the relay link show that resource partitioning is needed to obtain optimal performance when all the links are in operation. In particular, the resource allocation scheme described in this section has provided performance enhancement for the cell edge users while it has not increased average user throughput and total system capacity compared to the eNB-only scenario. This can be achieved with bandwidth scalability of 100 MHz supported by LTE-Advanced, more efficient resource allocation and frequency reuse scheme.

8 REFERENCES

[1]: 3GPP TR 25.913 v8.0.0, Requirements for Evolved UTRA (E-UTRA) and Evolved UTRAN (E-UTRAN) (Release 8), December 2008

[2]: H. Holma and A. Toskala, WCDMA for UMTS: HSPA Evolution and LTE, 4th Edition, Wiley 2007

[3]: E. Dahlman, S. Parkvall, J. Sköld and P. Beming, 3G Evolution HSPA and LTE for Mobile Broadband, Academic Press 2007

[4]: 3GPP TS 36.300 v8.7.0, E-UTRA and E-UTRAN; Overall Description; Stage 2 (Release 8), December 2008

[5]: A. Karaer, Analysis of FH-OFDMA Systems Hopping Patterns, Bachelor's Thesis, Helsinki University of Technology, June 2007

[6]: 3GPP TR 25.892 v6.0.0, Feasibility Study for Orthogonal Frequency Division Multiplexing (OFDM) for UTRAN enhancement (Release 6), June 2004

[7]: R. Van Nee and R. Prasad, OFDM for Wireless Multimedia Communications, Artech House, 2000

[8]: C. Gessner, UMTS Long Term Evolution (LTE) Technology Introduction, Rohde&Schwarz, 2007

[9]: 3GPP TS 36.211 v8.5.0, E-UTRA; Physical Channels and Modulation (Release 8), December 2008

[10]: H. G. Myung, J. Lim and D. J. Goodman, Single Carrier FDMA for Uplink Wireless Transmission, IEEE Vehicular Technology Magazine, vol. 1, no. 3, September 2006

[11]: R. Schoenen, Relay Based Access for Cellular: FDD versus TDD, Invited Presentation at IST Event 2006

[12]: R. Pabst, B.H Walke, D.C. Schultz, P. Herhold, H. Yanikomeroglu, S. Mukherjee, H. Viswanathan, M. Lott, W. Zirwas, M. Dohler, H. Aghvami, D.D. Falconer, G.P. Fettweis, Relay-Based Deployment Concepts for Wireless and Mobile Broadband Radio, IEEE Communications Magazine, September 2004

[13]: R1-082975, Application Scenarios for LTE-Advanced Relay, China Mobile, Huawei, Vodafone, TSG-RAN WG1 #54, Korea, August 2008

[14]: http://en.wikipedia.org/wiki/3GPP_Long_Term_Evolution

[15]: 3GPP TR 36.913 v8.0.0, Requirements for Further Advancements for E-UTRA (LTE-Advanced) Release 8, June 2008

[16]: 3GPP REV-080004, LTE-A-Proposals for Evolution, Nokia & Nokia Siemens Networks, TSG RAN IMT Advanced Workshop, China, April 2008

[17]: T. Beniero, S. Redana, J. Hämäläinen, B. Raaf, Effect of Relaying on Coverage in 3GPP LTE-Advanced, IEEE Vehicular Technology Conference (VTC) Spring, April 2009

[18]: 3GPP R1-084026, Text proposal for evaluation methodology, TSG-RAN WG1 #54bis, Czech Republic, October 2008

[19]: 3GPP TR 36.814 v0.3.1, Further Advancements for E-UTRA Physical Layer Aspects, 2008-2009

[20]: WINNER, "Wireless World Initiative New Radio", 2004-2007, http://www.ist-winner.org

[21]: IEEE802.16, "TSGj-Mobile Multihop Relaying (MMR)", 2007

[22]: M. Sawahashi, Radio Access Techniques for LTE-Advanced, Musashi Institute of Technology / NTT DOCOMO, INC., August 20, 2008

[23]: http://en.wikipedia.org/wiki/Power_control

[24]: 3GPP TR 25.814 v.7.1.0, Physical Layer Aspects for Evolved Universal Terrestrial Radio Access (Release 7), September 2006

[25]: C. Castellanos, D. L. Villa, C. Rosa, I. Z. Kov'acs, F. Frederiksen, and K. I. Pedersen, Performance of Fractional Power Control in UTRAN LTE Uplink, IEEE International Conference on Communications, Beijing, China, May 2008

[26]: A. Simonsson and A. Furuskar, Uplink Power Control in LTE - Overview and Performance, Wireless Access Networks, Ericsson Research, Vehicular Technology Conference, 2008. VTC 2008-Fall

[27]: M. Rao Anil, Reverse Link Power Control for Managing Inter-cell Interference in Orthogonal Multiple Access Systems, Vehicular Technology Conference, 2007. VTC-2007-Fall

[28]: 3GPP TS 36.213, v8.5.0, Evolved Universal Terrestrial Radio Access (E-UTRA) Physical Layer Procedures (Release 8), Tech. Report, December 2008

[29]: Winner II, Deliverable D3.5.1 v1.0, Relaying Concepts and Supporting Actions in the Context of CGs, October 2006

[30]: http://wireless.agilent.com/wireless/helpfiles/n7612b.htm, Physical Layer Structure, N7612B Signal Studio for TD-SCDMA, Agilent Technologies

[31]: 3GPP TS 36.423, v8.4.0, Evolved Universal Terrestrial Radio Access Network (E-UTRAN); X2 application protocol (X2AP) (Release 8), Tech. Report, December 2008